EXPERIMENTAL DETERMINATION OF THE REACTIVITY OF ISOPRENE WITH RESPECT TO OZONE FORMATION

Final Report for

UCAR Contract no. 59166

Roger Atkinson and William P. L. Carter
Principal Investigators

by

William P. L. Carter
John A Pierce
Irina L. Malkina
Dongmin Luo
William D. Long

January 28, 1993

Statewide Air Pollution Research Center
University of California
Riverside, California 92521-0312

ABSTRACT

A series of environmental chamber experiments were conducted to measure the effects of isoprene on ozone formation, NO oxidation, and OH radical levels in a simplified model photochemical smog system. The experiments consisted of repeated 6-hour irradiations of a simplified mixture of smog precursors, alternating with runs with varying amounts of isoprene added. The experiments were conducted at relatively low ROG/NO_x ratios to simulate conditions where VOCs have the greatest effect on ozone formation, and were carried out in conjunction with a larger program where similar data was obtained for 35 other types of VOCs. The amount of ozone formed and NO oxidized per isoprene reacted increased with reaction time, being approximately two molecules of ozone formed and NO oxidized per molecule of isoprene reacted in the first hour, and approximately four molecules in six hours, under the conditions of these experiments. Approximately half of this is estimated to be due directly to the reactions of isoprene and its oxidation products, while the other half is estimated to be due to the fact that isoprene increases the radical levels present in the system, causing additional ozone formation from the other VOCs present. Current atmospheric chemical mechanisms for isoprene, including a preliminary detailed isoprene mechanism, could not correctly simulate the results of these experiments.

PREFACE

The report describes work carried out at the Statewide Air Pollution Research Center (SAPRC) at the University of California at Riverside as a part of the Southern Oxidant Study (SOS). **This report is a draft which is being submitted for review. It has has not been approved for release as an SOS project output.**

The authors wish to acknowledge Dr. Roger Atkinson of SAPRC for assistance in administering this project and for helpful discussions. We also acknowledge Ms. Kathalema M. Smihula and Mr. Armando D. Avallone of the UCR College of Engineering, Center for Environmental Research and Technology (CE-CERT) for assistance in carrying out the experiments in this study. We thank Dr. Joseph Norbeck, director of CE-CERT, for supporting Ms. Smihula and Mr. Avallone during this period.

The opinions and conclusions in this report are entirely those of the authors. Mention of trade names and commercial products do not constitute endorsement or recommendation for use.

TABLE OF CONTENTS

LIST OF TABLES

LIST OF FIGURES

INTRODUCTION

The formation of ground-level ozone is a serious air pollution problem in many areas of the United States. Ozone is not emitted directly, but is formed from the photochemical interactions of emitted volatile organic compounds (VOCs) and oxides of nitrogen (NO_x). In order to reduce ground level ozone levels and achieve existing air quality standards, it is necessary to reduce emissions of both of these types of ozone precursors. VOC controls generally reduce the rate at which ozone is formed and thus have the greatest effects on the concentrations of ozone nearer the source areas, while NO_x controls generally reduce the ultimate amount of ozone which can be formed, and thus have the greatest effects on ozone downwind of the source areas. Traditionally ozone control strategies have focused on VOC controls because there are a wide variety of sources of VOCs, and because significant reductions of NO_x emissions have proven to be difficult and expensive. However, VOCs are emitted from biogenic as well as anthropogenic sources, and thus there is a certain component of the VOC emissions inventory which probably can never be completely controlled. Because of this it appears likely that the ground-level ozone pollution problem will not be solved unless significant new NO_x controls are also implemented. However, models predict that continued VOC control will have the greatest effect in reducing ozone near most of the urban centers, so VOC control will continue to be an important part of any comprehensive ozone control strategy.

In developing cost-effective VOC control strategies for reduction of ozone formation, it is critical to be able to quantify the effects of the naturally emitted VOCs which will not be controlled. It is also important to recognize that not all VOCs are equal in the amount of ozone formation they cause. The rate of reaction is clearly important, and if this were the only factor, the biogenic VOCs would be judged to be highly reactive. However, VOCs can also differ significantly on their effect on ozone formation even after differences in their rates of reaction are factored out. For example, Carter and Atkinson (1989) calculated that some VOCs can form five or more additional molecules of ozone being formed per molecule of VOC being reacted, while others form less than one molecule, and still others actually cause the amount of ozone formation to be reduced. Although the rates of reaction of most of the biogenic VOCs in the atmosphere have been determined, there presently are no experimental data concerning how much ozone is formed once they do react.

The effect of a VOC on ozone formation can be quantified by its "incremental reactivity". This is defined as the amount of additional ozone formation resulting from the addition of a small amount of the compound to the emissions in the episode, divided by the amount of compound added. The incremental reactivity of a VOC in an actual air pollution episode cannot be measured experimentally, except by making changes in emissions and observing changes in air quality under similar meteorological conditions. However, they can be calculated using computer airshed models if the VOC’s atmospheric reaction mechanism is known or can be estimated. (e.g., see Dodge, 1984; Carter and Atkinson, 1989; Chang and Rudy, 1990; Carter, 1991). However, such calculations are no more reliable than the model for the VOCs’ atmospheric chemical reactions. Therefore, experimental data are needed to test the ability of chemical mechanisms to reliably predict the incremental reactivities of VOCs of interest.

This report describes the results of a series of experiments to obtain the data needed to test the ability of models to predict the effects of isoprene on ozone formation under atmospheric conditions where VOC emissions have the greatest effect on ozone. Isoprene was chosen for initial study because it is believed to be the most important single emitted biogenic VOC, at least in the southern United States. Although the effects of VOCs on ozone depend significantly on environmental conditions, particularly NO_x levels, the initial experiments concerned the relatively high NO_x conditions because these are the conditions where VOCs have the greatest effect on ozone, and thus are the most relevant to the assessment of effects of VOC controls on ozone (Carter, 1991).

EXPERIMENTAL AND DATA ANALYSIS METHODS

This experimental study of isoprene reactivity was carried out as part of a much larger study of the reactivities of a variety of other VOCs, and the detailed methods of procedure and results are given in Appendix A to this report. This section gives a summary of the overall experimental approach and the methods used for data analysis.

General Approach

The reactivities of isoprene were measured by carrying out a series of repeated 6-hour irradiations of a standard mixture representing photochemical smog precursors in an indoor environmental chamber, alternating with irradiations of the same mixture with varying amounts of isoprene added. The ~3000 liter SAPRC indoor Teflon chamber #2, called the "ETC", was employed. The chamber consists of a flexible FEP Teflon bag held in a framework surrounded by blacklights which were used as the light source. Dry purified air for the experiments was provided by an in-house air purification system. The chamber was flushed with purified air overnight, and then the reactants were injected, mixed, and monitored. The blacklights were then turned on, and the chamber contents were irradiated for six hours. Ozone and NO_x were monitored continuously by commercial continuous analyzers, whose readings, along with the temperature data, were recorded on the data acquisition computer every 15 minutes. Organic reactants were monitored approximately hourly by gas chromatography. After the run the reaction bag chamber was deflated and flushed with pure air to remove the contents and prepare for the next run. Various types of characterization and control runs were also carried out from time to time; these are discussed in Appendix A.

The photochemical smog precursors utilized in the experiments consisted of a ~4.5 ppmC of a "mini-surrogate" reactive organic gas (ROG) mixture containing 35% (as carbon) ethene, 50% n-hexane, and 15% m-xylene, along with ~0.5 ppm of oxides of nitrogen (NO_x) in air. This was designed to represent "maximum reactivity" conditions, i.e., relatively low ROG/NO_x ratios where VOCs have the greatest effects on ozone formation (Carter, 1991). The 3-component mini-surrogate was designed to be an experimentally simple representative of the reactive organic compounds emitted into the atmosphere. Although this mini-surrogate is a significant oversimplification of the complex mixture of ROGs present in the atmosphere (see, for example, Jeffries et al. 1989), model calculations show that use of this simpler mixture provides a more sensitive measure of mechanistic reactivities than use of more complex mixtures.

The amount of VOCs added in the test experiments were varied, but generally the amount added was determined so that it caused at least a 40%, but less than a factor of 2, change in the sum of amount of NO consumed plus the amount of ozone formed in six hours. In the case of the isoprene experiments, the amount of isoprene ranged from 76 to 157 ppb, causing a 40-80% change in NO consumed and ozone formed.

A total of four experiments with added isoprene were carried out, each alternating with a standard ROG-NO_x-air experiment without the added isoprene. Since a large number of similar experiments were carried out with other VOCs added, this procedure resulted in a large number of replicates of the standard experiments being carried out. As discussed in Appendix A, this large number of standard runs is useful for determining the precision of the incremental reactivity measurements, and for controlling for the effects of run to run variability in the analysis of the effects of the added isoprene. Therefore, the results of all the relevant standard runs, not just those preceding or following the isoprene runs, were used in the analysis.

Data Analysis Methods

The results of the experiments with added isoprene, together with the results of the repeated standard runs, were analyzed to yield three measures of reactivity. The first was the effect of the added isoprene on the amount of NO reacted plus the amount of ozone formed at hourly intervals in the experiment. The amount of NO reacted plus the amount of ozone formed is referred to as d(O_3-NO). As discussed elsewhere (e.g., Johnson, 1983; Carter and Atkinson, 1987; Carter and Lurmann, 1990, 1991) this gives a direct measure of the amount of conversion of NO to NO_2 by peroxy radicals formed in the photooxidation reactions, which is the process that is directly responsible for ozone formation in the atmosphere. The incremental reactivity of the test VOC (e.g., isoprene) relative to d(O_3-NO) at time t, designated $IR[d(O_3\text{-}NO)]_t^{voc}$, is given by

$$IR[d(O_3\text{-}NO)]_t^{VOC} = \frac{d(O_3\text{-}NO)_t^{test} - d(O_3\text{-}NO)_t^{base}}{[VOC]_0} \qquad (I)$$

where $d(O_3\text{-}NO)_t^{test}$ is the d(O_3-NO) measured at time t from the experiment where the isoprene was added, $d(O_3\text{-}NO)_t^{base}$ is the corresponding value from the "base case" experiments where the isoprene was not present, and $[VOC]_0$ is the initial isoprene concentration in the experiment where it was added (i.e., the amount added). The incremental reactivity with respect to $d(O_3\text{-NO})$ was calculated for each hour of the experiment.

The second reactivity measure determined in this study is the effect of the isoprene on the integrated hydroxyl (OH) radical concentration in the experiment. The integrated OH radical concentration, referred to as IntOH, is derived from the fraction of the initially present m-xylene which reacts in the experiment, according to

$$\text{IntOH}_t = \frac{\ln\left(\frac{[\text{m-xyl}]_0}{[\text{m-xyl}]_t}\right) - Dt}{\text{kOH}^{\text{m-xyl}}}, \qquad \text{(II)}$$

where $[\text{m-xyl}]_0$ and $[\text{m-xyl}]_t$ are the initial and time=t concentrations of m-xylene, respectively, $\text{kOH}^{\text{m-xyl}}$ is the rate constant for the reaction of m-xylene with OH radicals, and D is the dilution rate in the experiments, which was estimated to be small but non-negligible (see Appendix A). The effect of the isoprene on IntOH was measured by its incremental reactivity relative to IntOH, or $\text{IR[IntOH]}_t^{\text{voc}}$, defined in a way exactly analogous to the incremental reactivity relative to $d(O_3\text{-NO})$:

$$\text{IR[IntOH]}_t^{\text{voc}} = \frac{\text{IntOH}_t^{\text{test}} - \text{IntOH}_t^{\text{base}}}{[\text{VOC}]_0} \qquad \text{(III)}$$

Reactivities relative to IntOH are also calculated at hourly intervals.

The third measure of reactivity obtained from the results of these experiments is a quantity we designate as the "direct reactivity", which is defined as:

$$\text{Direct Reactivity}^{\text{voc}} = \frac{d(O_3\text{-NO})^{\text{test}} - d(O_3\text{-NO})^{\text{base ROG (test)}}}{[\text{VOC}]_0} \qquad \text{(IV)}$$

where $d(O_3\text{-NO})^{\text{base ROG (test)}}$ is given by,

$$d(O_3\text{-NO})^{\text{base ROG (test)}} = \left(\frac{d(O_3\text{-NO})}{\text{IntOH}}\right)^{\text{base}} \text{IntOH}^{\text{test}} \qquad \text{(V)}$$

As discussed in Appendix A, $d(O_3\text{-NO})^{\text{base ROG (test)}}$ is the estimated amount of NO oxidized and ozone formed from the reactions of the base ROG surrogate components in the added test VOC run, and thus $d(O_3\text{-NO})^{\text{test}} - d(O_3\text{-NO})^{\text{base ROG (test)}}$ is the amount of ozone formed and NO oxidized estimated to be due to the direct reactions of the added VOC. Thus, the direct reactivity is sensitive to the amount of NO oxidation and ozone formation resulting directly from the test VOC's reactions, as opposed to the effect of the added VOC on how much ozone is formed and NO is oxidized from the reactions of the other ROGs present. If a compound has a strong effect on radical levels, i.e., has a high IntOH reactivity, it can have a significant effect on NO oxidation and ozone formation by affecting how rapidly the other VOCs present react and oxidize NO and form ozone. In such cases, the compound's $d(O_3\text{-}NO)$ reactivity is not sensitive to the amount of NO oxidation and ozone formation formed directly from the test VOC's reactions, and thus does not provide a good test for this aspect of the VOC's mechanism. On the other hand, the direct reactivity is sensitive to this aspect of the mechanism, and thus provides a useful tool for mechanism evaluation.

The quantities $d(O_3\text{-}NO)^{test}$, $IntOH^{test}$, and $[VOC]_0$ are obtained from the results of each of the individual experiments where a test VOC (e.g., isoprene) is added. However, because of run-to-run variability in temperature, light intensity, and initial reactant concentrations, the quantities $d(O_3\text{-}NO)^{base}$, $IntOH^{base}$, and $[d(O_3\text{-}NO)/IntOH]^{base}$ are not measured in a single experiment, but are estimates, based on the results of many base case runs, of what the result of the base case experiment would be if it were carried out under the conditions of the added test VOC experiment. These are obtained by linear multiple regression analyses on the results of the base case experiments as a function of the variable run conditions which were found to affect the result in the base case runs (see Appendix A). Because of the large number of VOCs studied under the higher NO_x, lower ROG/NO_x series, results from a total of 92 base case runs could be used to determine the base case estimates for these runs.The uncertainties in the estimates of the base case conditions from the regressions are used to estimate the uncertainties in the reactivities due to run-to-run variabilities which could not be accounted for by the regressions.

As discussed in Appendix A, a useful alternative measurement of reactivity which can be obtained from these data is what we term "mechanistic reactivities". Incremental reactivity can be thought of as being a product of two factors, the "kinetic reactivity", which is defined as the fraction of the emitted VOC which undergoes chemical reaction in the pollution scenario being considered,

$$\text{Kinetic Reactivity} = \text{Fraction Reacted} = \frac{\text{VOC Reacted}}{\text{VOC Added}}$$

and the "mechanistic reactivity", which is the amount of ozone formed relative to the amount of VOC which reacts in that scenario,

$$\text{Mechanistic Reactivity} = \frac{\text{Ozone Formed}}{\text{VOC Reacted}}$$

(Carter and Atkinson, 1987). The utility of this concept is that this provides a means to factor out (at least to a first approximation) the effect of a VOC's reaction rate from all the other mechanistic aspects which affect reactivity.

Since the only aspect of the VOCs mechanism which affects kinetic reactivities are the VOC's rate constants, which generally are known, the ability of a mechanism to predict kinetic reactivities are not considered to be particularly uncertain. On the other hand, the mechanistic reactivities are sensitive to all the other aspects of the VOC's mechanism, many (or all) of which are uncertain. For this reason, the mechanistic reactivities are the quantities of greatest interest to determine in these experiments.

Because of this, the discussion of these experiments, as well as most of the experiments in Appendix A, focus primarily on analysis of the data to yield mechanistic reactivities, and the ability of the mechanisms to simulate them. Mechanistic reactivities, or MR[d(O_3-NO)], MR[IntOH], and direct MR[d(O_3-NO)] (or ConvF — see below) are determined in an analogous way to incremental reactivities, except that (VOC reacted)$_t$, the amount of VOC reacted up to time=t, appears in the denominator of Equations (I), (III), and (IV), respectively, instead of $[VOC]_0$:

$$MR[d(O_3\text{-NO})]_t^{voc} = \frac{d(O_3\text{-NO})_t^{test} - d(O_3\text{-NO})_t^{base}}{[VOC\ reacted]_t} \qquad (VI)$$

$$MR[IntOH]_t^{voc} = \frac{IntOH_t^{test} - IntOH_t^{base}}{[VOC\ reacted]_t} \qquad (VII)$$

$$ConvF_t^{voc} = \frac{d(O_3\text{-NO})^{test} - d(O_3\text{-NO})^{base\ ROG\ (test)}}{[VOC\ reacted]_t} \qquad (VIII)$$

The direct mechanistic reactivity is called the "conversion factor", or "ConvF", because under high NO_x conditions the direct mechanistic reactivity is approximately equal to the number of NO conversions caused by the reactions of one molecule of the test VOC (see Appendix A).

The amounts of isoprene reacted at the various times in the experiment were determined by direct measurement. Most or all of the initially present isoprene reacted during the experiments, so by the end of the experiment the mechanistic reactivities were essentially the same as the incremental reactivities. However, this was not the case during the first several hours of the experiments.

MECHANISMS USED IN MODEL SIMULATIONS

The primary utility of these experiments is to provide data to test the ability of the chemical mechanisms used in airshed models to correctly predict the effects of emitted isoprene on NO oxidation, ozone formation, and radical levels in the atmosphere. Although a discussion of the development and characteristics of isoprene mechanisms is beyond the scope of this report, a series of model calculations were carried out to determine the extent to which these data are consistent with current mechanisms for isoprene’s atmospheric reactions. The chemical mechanisms used to simulate these experiments are listed and briefly discussed in this section.

Model simulation of reactivity experiments involves simulations of the base case experiment, then simulations of the same experiment with the test compound added, then analyzing the results using the same methodology as employed with the experimental data, as described above. These simulations thus require mechanisms for the compounds in the base case experiment (referred to as the "base case" mechanisms in the discussion below) as well as mechanisms for isoprene. They also require a model for the chamber effects and other run conditions in these experiments.

Two base case mechanisms were used in this study for the purpose of testing three different isoprene mechanisms. The "SAPRC-91" mechanism, discussed in Appendix A, was used to test the version of the isoprene mechanism which is included in the SAPRC-90 mechanism of Carter (1990), and was also used to test a preliminary detailed isoprene mechanism which we are developing. A slightly modified version of the Carbon Bond IV mechanism (Gery et al., 1988) was used to test the isoprene representation incorporated in that mechanism.

SAPRC-91 Base Case Mechanism

The SAPRC-91 base case mechanism used in this work is the same as the SAPRC-91 mechanism used in the model simulations discussed in Appendix A. This consists of a slightly updated and modified version of the "SAPRC-90" mechanism of Carter et al (1990). The aspects of the mechanism which were updated involved the kinetics of PAN formation and the photolysis of formaldehyde, and also several modifications were made to the mechanisms for m-xylene and the species representing its unknown photoreactive products. The unadjusted SAPRC mechanisms were found to somewhat underpredict the rate of ozone formation in the standard experiment in this study, and an adjustment had to be made to the m-xylene mechanism to yield acceptable fits to the data and to minimize possible biases being introduced into the reactivity simulations which might result if the mechanism could not simulate the results of the base case experiment. The species and reactions for this mechanisms are given in Tables 1 and 2, and the absorption cross sections and quantum yields which are different from those given by Carter (1990) are listed in Table 3.

Note that this mechanism is still in the process of being updated, and is subject to further modification before its documentation is published. In addition, the modified m-xylene mechanism it incorporates is considered to be suitable only for modeling the conditions of these experiments (see Appendix A).

SAPRC-90 Isoprene Mechanism

The SAPRC-90 mechanism of Carter (1990) uses a generalized parameter approach to represent the reactions of a wide variety of alkenes and other species, with isoprene being among the species for which parameter assignments are given. This mechanism in effect represents isoprene by using a model species which reacts with the appropriate OH, O_3, NO_3, and O^3P rate constants, but which form the same types of products as do the other alkenes once it reacts. Thus, the only species added to the mechanism to predict the reactivity of isoprene is isoprene itself; no new species are added to represent the reactions of isoprene’s products. This is similar to the approach used to represent isoprene in the RADM-2 chemical mechanism of Stockwell et al. (1990), and the performance of that mechanism is expected to be similar to the SAPRC-90 isoprene mechanism in simulating these data. The SAPRC-90 isoprene reactions are included with the listing of the SAPRC-91 mechanism on Table 2.

Preliminary Detailed Isoprene Mechanism

Under funding from a separate EPA program, we are in the process of developing a detailed mechanism for the reactions of isoprene and its major photooxidation products. This will then be used as the basis for developing improved condensed mechanisms for isoprene for use in airshed models. As part of this effort, a preliminary detailed mechanism for isoprene has been developed which has explicit representations for the reactions of its major primary and secondary reaction products. These known or expected products include methacrolein, methyl vinyl ketone, glycolaldehyde, hydroxyacetone, 3-methyl furan, and various C_5 hydroxy-methyl and methyl substituted acrolein species which we estimate are also formed (Carter, unpublished results — see also Paulson and Seinfeld, 1992). (The various C_5 hydroxy-substituted acroleins are

Table 1. List of Model Species Used in the SAPRC-91 Mechanism to Simulate the Reactivity of Isoprene

Name	Description
Constant Species.	
O2	Oxygen
M	Air
H2O	Water
Active Inorganic Species.	
O3	Ozone
NO	Nitric Oxide
NO2	Nitrogen Dioxide
NO3	Nitrate Radical
N2O5	Nitrogen Pentoxide
HONO	Nitrous Acid
HNO3	Nitric Acid
HNO4	Peroxynitric Acid
HO2H	Hydrogen Peroxide
Active Radical Species and Operators.	
HO2.	Hydroperoxide Radicals
RO2.	Operator to Calculate Total Organic Peroxy Radicals
RCO3.	Operator to Calculate Total Acetyl Peroxy Radicals
Active Reactive Organic Product Species.	
CO	Carbon Monoxide
HCHO	Formaldehyde
CCHO	Acetaldehyde
RCHO	Lumped C3+ Aldehydes
ACET	Acetone
MEK	Lumped Ketones
PHEN	Phenol
CRES	Cresols
BALD	Aromatic aldehydes (e.g., benzaldehyde)
GLY	Glyoxal
MGLY	Methyl Glyoxal
AFG1	Reactive Aromatic Fragmentation Products from benzene and naphthalene
AFG2	Other Reactive Aromatic Fragmentation Products.
RNO3	Organic Nitrates
NPHE	Nitrophenols
PAN	Peroxy Acetyl Nitrate
PPN	Peroxy Propionyl Nitrate
GPAN	PAN Analogue formed from Glyoxal
PBZN	PAN Analogues formed from Aromatic Aldehydes
-OOH	Operator Representing Hydroperoxy Groups.
Non-Reacting Species	
CO2	Carbon Dioxide
-C	"Lost Carbon"
-N	"Lost Nitrogen"
H2	Hydrogen

Table 1, (continued)

Name	Description
O3OL-SB	Operator used to account for total stabilized "Criegee biradical" formation. (When SO_2 is present, it is a steady-state species used to account for conversion of SO_2 to SO_3. Otherwise, it can be ignored.)
NOX-WALL	Counter species to account for NOx lost on walls, or (if negative) for NOx input coming off walls
Steady State Species and Operators.	
HO.	Hydroxyl Radicals
O	Ground State Oxygen Atoms
O*1D2	Excited Oxygen Atoms
RO2-R.	Peroxy Radical Operator representing NO to NO_2 conversion with HO_2 formation.
RO2-N.	Peroxy Radical Operator representing NO consumption with organic nitrate formation.
RO2-NP.	Peroxy Radical Operator representing NO consumption with nitrophenol formation
R2O2.	Peroxy Radical Operator representing NO to NO_2 conversion.
CCO-O2.	Peroxy Acetyl Radicals
C2CO-O2.	Peroxy Propionyl Radicals
HCOCO-O2.	Peroxyacyl Radical formed from Glyoxal
BZ-CO-O2.	Peroxyacyl Radical formed from Aromatic Aldehydes
HOCOO.	Intermediate formed in Formaldehyde + HO_2 reaction
BZ-O.	Phenoxy Radicals
BZ(NO2)-O.	Nitratophenoxy Radicals
HOCOO.	Radical Intermediate formed in the HO_2 + Formaldehyde system.
Mini-Surrogate Components and Related Species	
ETHE	Ethene
NC6	n-Hexane
MXYL	m-Xylene
MXYP	Product formed from m-Xylene in mini-surrogate instead of AFG2, for the m-xylene mechanism which is adjusted to fit the ETC Set 3 standard experiment.
Isoprene	
ISOP	Isoprene

Table 2. Listing of SAPRC-91 Mechanism as used to Simulate Results of Isoprene Reactivity Experiments. The SAPRC-90 Mechanism for Isoprene is also Shown.

Rxn. Label	Kinetic Parameters [a] k(300)	A	Ea	B	Reactions [b]
	COMMON REACTIONS IN SAPRC-91 MECHANISM				
Inorganic					
1	(Phot. Set = NO2)				NO2 + HV = NO + O
2	2.16E-05	2.16E-05	0.00	-4.30	O + O2 + M = O3 + M
3A	1.42E+04	9.54E+03	-0.24	-1.00	O + NO2 = NO + O2
3B	2.28E+03	(Falloff Kinetics)			O + NO2 = NO3 + M
	k0 =	3.23E-03	0.00	-4.00	
	kINF =	3.23E+04	0.00	-1.00	
		F= 0.60 n= 1.00			
4	2.76E+01	2.94E+03	2.78	-1.00	O3 + NO = NO2 + O2
5	4.94E-02	2.06E+02	4.97	-1.00	O3 + NO2 = O2 + NO3
6	4.11E+04	2.49E+04	-0.30	-1.00	NO + NO3 = #2 NO2
7	6.90E-10	1.19E-10	-1.05	-2.00	NO + NO + O2 = #2 NO2
8	1.84E+03	(Falloff Kinetics)			NO2 + NO3 = N2O5
	k0 =	7.90E-02	0.00	-6.30	
	kINF =	2.20E+03	0.00	-1.50	
		F= 0.60 n= 1.00			
9	2.26E-03	3.72E+13	22.26	1.00	N2O5 + #RCON8 = NO2 + NO3
10	1.47E-06	1.47E-06	0.00	-1.00	N2O5 + H2O = #2 HNO3
11	6.13E-01	3.67E+01	2.44	-1.00	NO2 + NO3 = NO + NO2 + O2
12A	(Phot. Set = NO3NO)				NO3 + HV = NO + O2
12B	(Phot. Set = NO3NO2)				NO3 + HV = NO2 + O
13A	(Phot. Set = O3O3P)				O3 + HV = O + O2
13B	(Phot. Set = O3O1D)				O3 + HV = O*1D2 + O2
14	3.23E+05	3.23E+05	0.00	-1.00	O*1D2 + H2O = #2 HO.
15	4.29E+04	2.82E+04	-0.25	-1.00	O*1D2 + M = O + M
16	7.05E+03	(Falloff Kinetics)			HO. + NO = HONO
	k0 =	2.51E-02	0.00	-4.60	
	kINF =	2.20E+04	0.00	-1.50	
		F= 0.60 n= 1.00			
17	(Phot. Set = HONO)				HONO + HV = HO. + NO
18	1.66E+04	(Falloff Kinetics)			HO. + NO2 = HNO3
	k0 =	9.34E-02	0.00	-5.20	
	kINF =	3.52E+04	0.00	-2.30	
		F= 0.60 n= 1.00			
19	1.51E+02	9.47E+00	-1.65	-1.00	HO. + HNO3 = H2O + NO3
21	3.52E+02	3.52E+02	0.00	-1.00	HO. + CO = HO2. + CO2
22	1.02E+02	2.35E+03	1.87	-1.00	HO. + O3 = HO2. + O2
23	1.21E+04	5.43E+03	-0.48	-1.00	HO2. + NO = HO. + NO2
24	2.00E+03	(Falloff Kinetics)			HO2. + NO2 = HNO4
	k0 =	6.46E-03	0.00	-5.20	
	kINF =	6.90E+03	0.00	-2.40	
		F= 0.60 n= 1.00			
25	3.24E-03	1.95E+13	21.66	1.00	HNO4 + #RCON24 = HO2. + NO2
27	6.77E+03	1.91E+03	-0.75	-1.00	HNO4 + HO. = H2O + NO2 + O2
28	3.05E+00	1.61E+01	0.99	-1.00	HO2. + O3 = HO. + #2 O2
29A	2.54E+03	3.23E+02	-1.23	-1.00	HO2. + HO2. = HO2H + O2
29B	1.80E-03	6.82E-05	-1.95	-2.00	HO2. + HO2. + M = HO2H + O2
29C	1.34E-01	1.11E-05	-5.60	-2.00	HO2. + HO2. + H2O = HO2H + O2 + H2O
29D	9.52E-02	2.37E-06	-6.32	-2.00	HO2. + HO2. + H2O = HO2H + O2 + H2O
30A	(Same k as Reaction 29A)				NO3 + HO2. = HNO3 + O2
30B	(Same k as Reaction 29B)				NO3 + HO2. + M = HNO3 + O2
30C	(Same k as Reaction 29C)				NO3 + HO2. + H2O = HNO3 + O2 + H2O
30D	(Same k as Reaction 29D)				NO3 + HO2. + H2O = HNO3 + O2 + H2O
31	(Phot. Set = H2O2)				HO2H + HV = #2 HO.
32	2.49E+03	4.84E+03	0.40	-1.00	HO2H + HO. = HO2. + H2O
33	1.45E+05	6.75E+04	-0.46	-1.00	HO. + HO2. = H2O + O2
General Peroxy					
B1	1.13E+04	6.16E+03	-0.36	-1.00	RO2. + NO = NO
B2	3.31E+04	(Falloff Kinetics)			RCO3. + NO = NO
	k0 =	2.03E+01	0.00	-9.10	
	kINF =	3.87E+04	0.00	-1.90	
		F= 0.27 n= 1.00			
B4	1.52E+04	(Falloff Kinetics)			RCO3. + NO2 = NO2
	k0 =	9.23E+00	0.00	-9.10	
	kINF =	1.76E+04	0.00	-1.90	
		F= 0.30 n= 1.00			
B5	7.19E+03	4.99E+02	-1.59	-1.00	RO2. + HO2. = HO2.
B6	7.19E+03	4.99E+02	-1.59	-1.00	RCO3. + HO2. = HO2.
B8	1.47E+00	1.47E+00	0.00	-1.00	RO2. + RO2. =
B9	1.60E+04	2.73E+03	-1.05	-1.00	RO2. + RCO3. =
B10	2.40E+04	4.11E+03	-1.05	-1.00	RCO3. + RCO3. =

Table 2 (continued)

Rxn. Label	k(300)	A	Ea	B	Reactions [b]
B11	(Same k as Reaction B1)				RO2-R. + NO = NO2 + HO2.
B12	(Same k as Reaction B5)				RO2-R. + HO2. = -OOH
B13	(Same k as Reaction B8)				RO2-R. + RO2. = RO2. + #.5 HO2.
B14	(Same k as Reaction B9)				RO2-R. + RCO3. = RCO3. + #.5 HO2.
B19	(Same k as Reaction B1)				RO2-N. + NO = RNO3
B20	(Same k as Reaction B5)				RO2-N. + HO2. = -OOH + MEK + #1.5 -C
B21	(Same k as Reaction B8)				RO2-N. + RO2. = RO2. + #.5 HO2. + MEK + #1.5 -C
B22	(Same k as Reaction B9)				RO2-N. + RCO3. = RCO3. + #.5 HO2. + MEK + #1.5 -C
B15	(Same k as Reaction B1)				R2O2. + NO = NO2
B16	(Same k as Reaction B5)				R2O2. + HO2. =
B17	(Same k as Reaction B8)				R2O2. + RO2. = RO2.
B18	(Same k as Reaction B9)				R2O2. + RCO3. = RCO3.
B23	(Same k as Reaction B1)				RO2-XN. + NO = -N
B24	(Same k as Reaction B5)				RO2-XN. + HO2. = -OOH
B25	(Same k as Reaction B8)				RO2-XN. + RO2. = RO2. + #.5 HO2.
B26	(Same k as Reaction B9)				RO2-XN. + RCO3. = RCO3. + HO2.
G2	(Same k as Reaction B1)				RO2-NP. + NO = NPHE
G3	(Same k as Reaction B5)				RO2-NP. + HO2. = -OOH + #6 -C
G4	(Same k as Reaction B8)				RO2-NP. + RO2. = RO2. + #.5 HO2. + #6 -C
G5	(Same k as Reaction B9)				RO2-NP. + RCO3. = RCO3. + HO2. + #6 -C
Common Organic Products					
B7	(Phot. Set = CO2H)				-OOH + HV = HO2. + HO.
B7A	2.65E+03	1.73E+03	-0.25	-1.00	HO. + -OOH = HO.
B7B	5.45E+03	2.63E+03	-0.44	-1.00	HO. + -OOH = RO2-R. + RO2.
C1	(Phot. Set = HCHONEWR)				HCHO + HV = #2 HO2. + CO
C2	(Phot. Set = HCHONEWM)				HCHO + HV = H2 + CO
C3	1.43E+04	1.65E+03	-1.29	1.00	HCHO + HO. = HO2. + CO + H2O
C4	1.14E+02	1.42E+01	-1.24	-1.00	HCHO + HO2. = HOCOO.
C4A	1.06E+04	1.44E+14	13.91	0.00	HOCOO. = HO2. + HCHO
C4B	(Same k as Reaction B1)				HOCOO. + NO = -C + NO2 + HO2.
C9	9.36E-01	4.11E+03	5.00	-1.00	HCHO + NO3 = HNO3 + HO2. + CO
C10	2.30E+04	8.15E+03	-0.62	-1.00	CCHO + HO. = CCO-O2. + H2O + RCO3.
C11A	(Phot. Set = CCHOR)				CCHO + HV = CO + HO2. + HCHO + RO2-R. + RO2.
C12	4.17E+00	2.05E+03	3.70	-1.00	CCHO + NO3 = HNO3 + CCO-O2. + RCO3.
C25	2.89E+04	1.25E+04	-0.50	-1.00	RCHO + HO. = C2CO-O2. + RCO3.
C26	(Phot. Set = RCHO)				RCHO + HV = CCHO + RO2-R. + RO2. + CO + HO2.
C27	4.17E+00	2.05E+03	3.70	-1.00	NO3 + RCHO = HNO3 + C2CO-O2. + RCO3.
C38	3.39E+02	2.82E+02	-0.11	1.00	ACET + HO. = #.8 "MGLY + RO2-R." + #.2 "R2O2. + HCHO + CCO-O2. + RCO3." + RO2.
C39	(Phot. Set = ACETONE)				ACET + HV = CCO-O2. + HCHO + RO2-R. + RCO3. + RO2.
C44	1.70E+03	4.29E+02	-0.82	1.00	MEK + HO. = H2O + #.5 "CCHO + HCHO + CCO-O2. + C2CO-O2." + RCO3. + #1.5 "R2O2. + RO2."
C57	(Phot. Set = KETONE)				MEK + HV + #.1 = CCO-O2. + CCHO + RO2-R. + RCO3. + RO2.
C95	3.03E+03	3.22E+04	1.41	-1.00	RNO3 + HO. = NO2 + #.155 MEK + #1.05 RCHO + #.48 CCHO + #.16 HCHO + #.11 -C + #1.39 "R2O2. + RO2."
C68A	(Phot. Set = MEGLYOX1)				MGLY + HV = HO2. + CO + CCO-O2. + RCO3.
C68B	(Phot. Set = MEGLYOX2)				MGLY + HV + #.107 = HO2. + CO + CCO-O2. + RCO3.
C69	2.52E+04	2.52E+04	0.00	-1.00	MGLY + HO. = CO + CCO-O2. + RCO3.
C70	(Same k as Reaction C12)				MGLY + NO3 = HNO3 + CO + CCO-O2. + RCO3.
C13	(Same k as Reaction B2)				CCO-O2. + NO = CO2 + NO2 + HCHO + RO2-R. + RO2.
C14	(Same k as Reaction B4)				CCO-O2. + NO2 = PAN
C15	(Same k as Reaction B6)				CCO-O2. + HO2. = -OOH + CO2 + HCHO
C16	(Same k as Reaction B9)				CCO-O2. + RO2. = RO2. + #.5 HO2. + CO2 + HCHO
C17	(Same k as Reaction B10)				CCO-O2. + RCO3. = RCO3. + HO2. + CO2 + HCHO
C18	3.90E-02	(Falloff Kinetics)			PAN = CCO-O2. + NO2 + RCO3.
	k0 =	7.19E+12	23.97	-1.00	
	kINF =	2.40E+18	27.08	0.00	
		F= 0.30 n= 1.00			
C28	(Same k as Reaction B2)				C2CO-O2. + NO = CCHO + RO2-R. + CO2 + NO2 + RO2.
C29	1.23E+04	0.00	-1.00		C2CO-O2. + NO2 = PPN
C30	(Same k as Reaction B6)				C2CO-O2. + HO2. = -OOH + CCHO + CO2
C31	(Same k as Reaction B9)				C2CO-O2. + RO2. = RO2. + #.5 HO2. + CCHO + CO2

Table 2 (continued)

Rxn. Label	Kinetic Parameters [a]				Reactions [b]
	k(300)	A	Ea	B	
C32	(Same k as Reaction B10)				C2CO-O2. + RCO3. = RCO3. + HO2. + CCHO + CO2
C33	4.07E-02	9.60E+18	27.97	0.00	PPN = C2CO-O2. + NO2 + RCO3.
C58A	(Phot. Set = GLYOXAL1)				GLY + HV = #.8 HO2. + #.45 HCHO + #1.55 CO
C58B	(Phot. Set = GLYOXAL2)				GLY + HV + #0.029 = #.13 HCHO + #1.87 CO
C59	1.67E+04	1.67E+04	0.00	-1.00	GLY + HO. = #.6 HO2. + #1.2 CO + #.4 "HCOCO-O2. + RCO3."
C60	(Same k as Reaction C12)				GLY + NO3 = HNO3 + #.6 HO2. + #1.2 CO + #.4 "HCOCO-O2. + RCO3."
C62	(Same k as Reaction B2)				HCOCO-O2. + NO = NO2 + CO2 + CO + HO2.
C63	(Same k as Reaction B4)				HCOCO-O2. + NO2 = GPAN
C64	(Same k as Reaction C18)				GPAN = HCOCO-O2. + NO2 + RCO3.
C65	(Same k as Reaction B6)				HCOCO-O2. + HO2. = -OOH + CO2 + CO
C66	(Same k as Reaction B9)				HCOCO-O2. + RO2. = RO2. + #.5 HO2. + CO2 + CO
C67	(Same k as Reaction B10)				HCOCO-O2. + RCO3. = RCO3. + HO2. + CO2 + CO
G46	3.86E+04	3.86E+04	0.00	-1.00	HO. + PHEN = #.15 RO2-NP. + #.85 RO2-R. + #.2 GLY + #4.7 -C + RO2.
G51	5.28E+03	5.28E+03	0.00	-1.00	NO3 + PHEN = HNO3 + BZ-O.
G52	6.16E+04	6.16E+04	0.00	-1.00	HO. + CRES = #.15 RO2-NP. + #.85 RO2-R. + #.2 MGLY + #5.5 -C + RO2.
G57	3.08E+04	3.08E+04	0.00	-1.00	NO3 + CRES = HNO3 + BZ-O. + -C
G30	1.89E+04	1.89E+04	0.00	-1.00	BALD + HO. = BZ-CO-O2. + RCO3.
G31	(Phot. Set = BZCHO)				BALD + HV + #.05 = #7 -C
G32	3.83E+00	2.05E+03	3.75	-1.00	BALD + NO3 = HNO3 + BZ-CO-O2.
G33	(Same k as Reaction B2)				BZ-CO-O2. + NO = BZ-O. + CO2 + NO2 + R2O2. + RO2.
G34	1.23E+04	1.23E+04	0.00	-1.00	BZ-CO-O2. + NO2 = PBZN
G36	(Same k as Reaction B6)				BZ-CO-O2. + HO2. = -OOH + CO2 + PHEN
G37	(Same k as Reaction B9)				BZ-CO-O2. + RO2. = RO2. + #.5 HO2. + CO2 + PHEN
G38	(Same k as Reaction B10)				BZ-CO-O2. + RCO3. = RCO3. + HO2. + CO2 + PHEN
G35	1.30E-02	9.60E+16	25.90	0.00	PBZN = BZ-CO-O2. + NO2 + RCO3.
G43	5.19E+04	1.91E+04	-0.60	-1.00	BZ-O. + NO2 = NPHE
G44	(Same k as Reaction B5)				BZ-O. + HO2. = PHEN
G45	6.00E-02	(No T Dependence)			BZ-O. = PHEN
G58	5.28E+03	5.28E+03	0.00	-1.00	NPHE + NO3 = HNO3 + BZ(NO2)-O.
G59	(Same k as Reaction G43)				BZ(NO2)-O. + NO2 = #2 -N + #6 -C
G60	(Same k as Reaction B5)				BZ(NO2)-O. + HO2. = NPHE
G61	(Same k as Reaction G45)				BZ(NO2)-O. = NPHE
					(See note [c])
G7	1.67E+04	1.67E+04	0.00	-1.00	HO. + AFG1 = HCOCO-O2. + RCO3.
G8	(Phot. Set = ACROLEIN)				AFG1 + HV + #.029 = HO2. + HCOCO-O2. + RCO3.
U1O3	0.00E+00	0.00E+00	0.00	-1.00	AFG1 + O3 = #.5 "HCHO + GLY + -C" + HO2.
G9	2.52E+04	2.52E+04	0.00	-1.00	HO. + AFG2 = C2CO-O2. + RCO3.
G10	(Phot. Set = ACROLEIN)				AFG2 + HV = HO2. + CO + CCO-O2. + RCO3.
					REACTIONS OF MINI-SURROGATE COMPONENTS (m-Xylene mechanism applicable for these runs **only**)
D1	1.24E+04	2.88E+03	-0.87	-1.00	ETHE + HO. = #.22 CCHO + #1.56 HCHO + RO2-R. + RO2.
D6	2.75E-03	1.76E+01	5.23	-1.00	ETHE + O3 = HCHO + #.37 O3OL-SB + #.44 CO + #.56 -C + #.12 HO2.
D8	1.09E+03	1.53E+04	1.57	-1.00	ETHE + O = HCHO + CO + HO2. + RO2-R. + RO2.
D9	3.16E-01	7.97E+03	6.04	-1.00	ETHE + NO3 = NO2 + #2 HCHO + R2O2. + RO2.
C6OH	8.27E+03	1.98E+04	0.52	-1.00	NC6 + HO. = #.815 RO2-R. + #.185 RO2-N. + #.74 R2O2. + #1.74 RO2. + #.020 CCHO + #.105 RCHO + #1.134 MEK + #.186 -C
MXOH	3.46E+04	3.46E+04	0.00	-1.00	MXYL + HO. = #.82 RO2-R. + #.18 HO2. + #.82 RO2. + #.18 CRES + #.04 BALD + #.108 GLY + #.37 MGLY + #2 MXYP + #-8.866 -C
MXP1	2.52E+04	2.52E+04	0.00	-1.00	HO. + MXYP = C2CO-O2. + RCO3.
MXP2	(Phot. Set = ACROLEIN)				MXYP + HV + #.22 = HO2. + CO + CCO-O2. + RCO3.
					CHAMBER-DEPENDENT REACTIONS (Applicable for these ETC runs only)
O3W	3.70E-04	(No T Dependence)			O3 =
N25I	2.50E-03	(No T Dependence)			N2O5 = #2 NOX-WALL
N25S	5.00E-08	0.00E+00	0.00	-1.00	N2O5 + H2O = #2 NOX-WALL
NO2W	1.40E-04	(No T Dependence)			NO2 = #.2 HONO + #.8 NOX-WALL
RSI	(Phot. Set = NO2)				HV + #2.E-5 = HO.
ONO2	(Phot. Set = NO2)				HV + #1.E-4 = NO2 + #-1 NOX-WALL
XSHC	2.50E+02	(No T Dependence)			HO. = HO2.

Table 2 (continued)

Rxn. Label	Kinetic Parameters [a]				Reactions [b]
	k(300)	A	Ea	B	
					SAPRC-90 ISOPRENE MECHANISM
ISOH	9.97E-11	2.54E-11	-0.81	0.00	ISOP + HO. = RO2-R. + RO2. + HCHO + RCHO + -C
ISO3	1.50E-17	1.23E-14	4.00	0.00	ISOP + O3 = #.135 RO2-R. + #.165 HO2. + #.135 RO2. + #.5 HCHO + #.15 CCHO + #.5 RCHO + #.21 MEK + #.295 CO + #1.565 -C + #.06 HO. + #.285 O3OL-SB + #.36 OLE-RI
ISN3	6.85E-13	3.03E-12	0.89	0.00	ISOP + NO3 = R2O2. + RO2. + HCHO + RCHO + -C + NO2
ISOA	6.00E-11	(No T Dependence)			ISOP + O = #.4 HO2. + #.5 RCHO + #.5 MEK + #1.5 -C + #.4 OLE-RI

[a] Except as noted, expression for rate constant is $k = A\ e^{Ea/RT}\ (T/300)^{B}$. Rate constants and A factor are in ppm, min units. Units of Ea is kcal $mole^{-1}$. "Phot Set" means this is a photolysis reaction, with the absorption coefficients and quantum yields given in Carter (1990) or in Table ?.

[b] Format of reaction listing same as used in documentation of the detailed mechanism (Carter 1990).

[c] AFG1 and AFG2 are not formed in the mini-surrogate or mini-surrogate + isoprene experiments. Their reactions are included here because they are among the common products in the SAPRC-91 mechanism.

Table 3. Absorption Cross Sections and Quantum Yields for Photolysis Reactions in the SAPRC-90 Mechanism which are not in the mechanism of Carter (1990).

WL (nm)	Abs (cm^2)	QY	WL (nm)	Abs (cm^2)	QY	WL (nm)	Abs (cm^2)	QY	WL (nm)	Abs (cm^2)	QY	WL (nm)	Abs (cm^2)	QY
Photolysis File = ACROLEIN														
250.0	1.80E-21	1.000	252.0	2.05E-21	1.000	253.0	2.20E-21	1.000	254.0	2.32E-21	1.000	255.0	2.45E-21	1.000
256.0	2.56E-21	1.000	257.0	2.65E-21	1.000	258.0	2.74E-21	1.000	259.0	2.83E-21	1.000	260.0	2.98E-21	1.000
261.0	3.24E-21	1.000	262.0	3.47E-21	1.000	263.0	3.58E-21	1.000	264.0	3.93E-21	1.000	265.0	4.67E-21	1.000
266.0	5.10E-21	1.000	267.0	5.38E-21	1.000	268.0	5.73E-21	1.000	269.0	6.13E-21	1.000	270.0	6.64E-21	1.000
271.0	7.20E-21	1.000	272.0	7.77E-21	1.000	273.0	8.37E-21	1.000	274.0	8.94E-21	1.000	275.0	9.55E-21	1.000
276.0	1.04E-20	1.000	277.0	1.12E-20	1.000	278.0	1.19E-20	1.000	279.0	1.27E-20	1.000	280.0	1.27E-20	1.000
281.0	1.26E-20	1.000	282.0	1.26E-20	1.000	283.0	1.28E-20	1.000	284.0	1.33E-20	1.000	285.0	1.38E-20	1.000
286.0	1.44E-20	1.000	287.0	1.50E-20	1.000	288.0	1.57E-20	1.000	289.0	1.63E-20	1.000	290.0	1.71E-20	1.000
291.0	1.78E-20	1.000	292.0	1.86E-20	1.000	293.0	1.95E-20	1.000	294.0	2.05E-20	1.000	295.0	2.15E-20	1.000
296.0	2.26E-20	1.000	297.0	2.37E-20	1.000	298.0	2.48E-20	1.000	299.0	2.60E-20	1.000	300.0	2.73E-20	1.000
301.0	2.85E-20	1.000	302.0	2.99E-20	1.000	303.0	3.13E-20	1.000	304.0	3.27E-20	1.000	305.0	3.39E-20	1.000
306.0	3.51E-20	1.000	307.0	3.63E-20	1.000	308.0	3.77E-20	1.000	309.0	3.91E-20	1.000	310.0	4.07E-20	1.000
311.0	4.25E-20	1.000	312.0	4.39E-20	1.000	313.0	4.44E-20	1.000	314.0	4.50E-20	1.000	315.0	4.59E-20	1.000
316.0	4.75E-20	1.000	317.0	4.90E-20	1.000	318.0	5.05E-20	1.000	319.0	5.19E-20	1.000	320.0	5.31E-20	1.000
321.0	5.43E-20	1.000	322.0	5.52E-20	1.000	323.0	5.60E-20	1.000	324.0	5.67E-20	1.000	325.0	5.67E-20	1.000
326.0	5.62E-20	1.000	327.0	5.63E-20	1.000	328.0	5.71E-20	1.000	329.0	5.76E-20	1.000	330.0	5.80E-20	1.000
331.0	5.95E-20	1.000	332.0	6.23E-20	1.000	333.0	6.39E-20	1.000	334.0	6.38E-20	1.000	335.0	6.24E-20	1.000
336.0	6.01E-20	1.000	337.0	5.79E-20	1.000	338.0	5.63E-20	1.000	339.0	5.56E-20	1.000	340.0	5.52E-20	1.000
341.0	5.54E-20	1.000	342.0	5.53E-20	1.000	343.0	5.47E-20	1.000	344.0	5.41E-20	1.000	345.0	5.40E-20	1.000
346.0	5.48E-20	1.000	347.0	5.90E-20	1.000	348.0	6.08E-20	1.000	349.0	6.00E-20	1.000	350.0	5.53E-20	1.000
351.0	5.03E-20	1.000	352.0	4.50E-20	1.000	353.0	4.03E-20	1.000	354.0	3.75E-20	1.000	355.0	3.55E-20	1.000
356.0	3.45E-20	1.000	357.0	3.46E-20	1.000	358.0	3.49E-20	1.000	359.0	3.41E-20	1.000	360.0	3.23E-20	1.000
361.0	2.95E-20	1.000	362.0	2.81E-20	1.000	363.0	2.91E-20	1.000	364.0	3.25E-20	1.000	365.0	3.54E-20	1.000
366.0	3.30E-20	1.000	367.0	2.78E-20	1.000	368.0	2.15E-20	1.000	369.0	1.59E-20	1.000	370.0	1.19E-20	1.000
371.0	8.99E-21	1.000	372.0	7.22E-21	1.000	373.0	5.86E-21	1.000	374.0	4.69E-21	1.000	375.0	3.72E-21	1.000
376.0	3.57E-21	1.000	377.0	3.55E-21	1.000	378.0	2.83E-21	1.000	379.0	1.69E-21	1.000	380.0	8.29E-24	1.000
381.0	0.00E+00	1.000												
Photolysis File = HCHONEWR														
280.0	2.49E-20	0.590	280.5	1.42E-20	0.596	281.0	1.51E-20	0.602	281.5	1.32E-20	0.608	282.0	9.73E-21	0.614
282.5	6.76E-21	0.620	283.0	5.82E-21	0.626	283.5	9.10E-21	0.632	284.0	3.71E-20	0.638	284.5	4.81E-20	0.644
285.0	3.95E-20	0.650	285.5	2.87E-20	0.656	286.0	2.24E-20	0.662	286.5	1.74E-20	0.668	287.0	1.13E-20	0.674
287.5	1.10E-20	0.680	288.0	2.62E-20	0.686	288.5	4.00E-20	0.692	289.0	3.55E-20	0.698	289.5	2.12E-20	0.704
290.0	1.07E-20	0.710	290.5	1.35E-20	0.713	291.0	1.99E-20	0.717	291.5	1.56E-20	0.721	292.0	8.65E-21	0.724
292.5	5.90E-21	0.727	293.0	1.11E-20	0.731	293.5	6.26E-20	0.735	294.0	7.40E-20	0.738	294.5	5.36E-20	0.741
295.0	4.17E-20	0.745	295.5	3.51E-20	0.749	296.0	2.70E-20	0.752	296.5	1.75E-20	0.755	297.0	1.16E-20	0.759
297.5	1.51E-20	0.763	298.0	3.69E-20	0.766	298.5	4.40E-20	0.769	299.0	3.44E-20	0.773	299.5	2.02E-20	0.776
300.0	1.06E-20	0.780	300.4	7.01E-21	0.780	300.6	8.63E-21	0.779	300.8	1.47E-20	0.779	301.0	2.01E-20	0.779
301.2	2.17E-20	0.779	301.4	1.96E-20	0.779	301.6	1.54E-20	0.778	301.8	1.26E-20	0.778	302.0	1.03E-20	0.778
302.2	8.53E-21	0.778	302.4	7.13E-21	0.778	302.6	6.61E-21	0.777	302.8	1.44E-20	0.777	303.0	3.18E-20	0.777
303.2	3.81E-20	0.777	303.4	5.57E-20	0.777	303.6	6.91E-20	0.776	303.8	6.58E-20	0.776	304.0	6.96E-20	0.776
304.2	5.79E-20	0.776	304.4	5.24E-20	0.776	304.6	4.30E-20	0.775	304.8	3.28E-20	0.775	305.0	3.60E-20	0.775
305.2	5.12E-20	0.775	305.4	4.77E-20	0.775	305.6	4.43E-20	0.774	305.8	4.60E-20	0.774	306.0	4.01E-20	0.774
306.2	3.28E-20	0.774	306.4	2.66E-20	0.774	306.6	2.42E-20	0.773	306.8	1.95E-20	0.773	307.0	1.58E-20	0.773
307.2	1.37E-20	0.773	307.4	1.19E-20	0.773	307.6	1.01E-20	0.772	307.8	9.01E-21	0.772	308.0	8.84E-21	0.772
308.2	2.08E-20	0.772	308.4	2.39E-20	0.772	308.6	3.08E-20	0.771	308.8	3.39E-20	0.771	309.0	3.18E-20	0.771
309.2	3.06E-20	0.771	309.4	2.84E-20	0.771	309.6	2.46E-20	0.770	309.8	1.95E-20	0.770	310.0	1.57E-20	0.770
310.2	1.26E-20	0.767	310.4	9.26E-21	0.764	310.6	7.71E-21	0.761	310.8	6.05E-21	0.758	311.0	5.13E-21	0.755
311.2	4.82E-21	0.752	311.4	4.54E-21	0.749	311.6	6.81E-21	0.746	311.8	1.04E-20	0.743	312.0	1.43E-20	0.740

Table 3. (continued)

Photolysis File = HCHONEWR (continued)

WL (nm)	Abs (cm^2)	QY	WL (nm)	Abs (cm^2)	QY	WL (nm)	Abs (cm^2)	QY	WL (nm)	Abs (cm^2)	QY	WL (nm)	Abs (cm^2)	QY
312.2	1.47E-20	0.737	312.4	1.35E-20	0.734	312.6	1.13E-20	0.731	312.8	9.86E-21	0.728	313.0	7.82E-21	0.725
313.2	6.48E-21	0.722	313.4	1.07E-20	0.719	313.6	2.39E-20	0.716	313.8	3.80E-20	0.713	314.0	5.76E-20	0.710
314.2	6.14E-20	0.707	314.4	7.45E-20	0.704	314.6	5.78E-20	0.701	314.8	5.59E-20	0.698	315.0	4.91E-20	0.695
315.2	4.37E-20	0.692	315.4	3.92E-20	0.689	315.6	2.89E-20	0.686	315.8	2.82E-20	0.683	316.0	2.10E-20	0.680
316.2	1.66E-20	0.677	316.4	2.05E-20	0.674	316.6	4.38E-20	0.671	316.8	5.86E-20	0.668	317.0	6.28E-20	0.665
317.2	5.07E-20	0.662	317.4	4.33E-20	0.659	317.6	4.17E-20	0.656	317.8	3.11E-20	0.653	318.0	2.64E-20	0.650
318.2	2.24E-20	0.647	318.4	1.70E-20	0.644	318.6	1.24E-20	0.641	318.8	1.11E-20	0.638	319.0	7.70E-21	0.635
319.2	6.36E-21	0.632	319.4	5.36E-21	0.629	319.6	4.79E-21	0.626	319.8	6.48E-21	0.623	320.0	1.48E-20	0.620
320.2	1.47E-20	0.614	320.4	1.36E-20	0.608	320.6	1.69E-20	0.601	320.8	1.32E-20	0.595	321.0	1.49E-20	0.589
321.2	1.17E-20	0.583	321.4	1.15E-20	0.577	321.6	9.64E-21	0.570	321.8	7.26E-21	0.564	322.0	5.94E-21	0.558
322.2	4.13E-21	0.552	322.4	3.36E-21	0.546	322.6	2.39E-21	0.539	322.8	2.01E-21	0.533	323.0	1.76E-21	0.527
323.2	2.82E-21	0.521	323.4	4.65E-21	0.515	323.6	7.00E-21	0.508	323.8	7.80E-21	0.502	324.0	7.87E-21	0.496
324.2	6.59E-21	0.490	324.4	5.60E-21	0.484	324.6	4.66E-21	0.477	324.8	4.21E-21	0.471	325.0	7.77E-21	0.465
325.2	2.15E-20	0.459	325.4	3.75E-20	0.453	325.6	4.10E-20	0.446	325.8	6.47E-20	0.440	326.0	7.59E-20	0.434
326.2	6.51E-20	0.428	326.4	5.53E-20	0.422	326.6	5.76E-20	0.415	326.8	4.43E-20	0.409	327.0	3.44E-20	0.403
327.2	3.22E-20	0.397	327.4	2.13E-20	0.391	327.6	1.91E-20	0.384	327.8	1.42E-20	0.378	328.0	9.15E-21	0.372
328.2	6.79E-21	0.366	328.4	4.99E-21	0.360	328.6	4.77E-21	0.353	328.8	1.75E-20	0.347	329.0	3.27E-20	0.341
329.2	3.99E-20	0.335	329.4	5.13E-20	0.329	329.6	4.00E-20	0.322	329.8	3.61E-20	0.316	330.0	3.38E-20	0.310
330.2	3.08E-20	0.304	330.4	2.16E-20	0.298	330.6	2.09E-20	0.291	330.8	1.41E-20	0.285	331.0	9.95E-21	0.279
331.2	7.76E-21	0.273	331.4	6.16E-21	0.267	331.6	4.06E-21	0.260	331.8	3.03E-21	0.254	332.0	2.41E-21	0.248
332.2	1.74E-21	0.242	332.4	1.33E-21	0.236	332.6	2.70E-21	0.229	332.8	1.65E-21	0.223	333.0	1.17E-21	0.217
333.2	9.84E-22	0.211	333.4	8.52E-22	0.205	333.6	6.32E-22	0.198	333.8	5.21E-22	0.192	334.0	1.46E-21	0.186
334.2	1.80E-21	0.180	334.4	1.43E-21	0.174	334.6	1.03E-21	0.167	334.8	7.19E-22	0.161	335.0	4.84E-22	0.155
335.2	2.73E-22	0.149	335.4	1.34E-22	0.143	335.6	-1.62E-22	0.136	335.8	1.25E-22	0.130	336.0	4.47E-22	0.124
336.2	1.23E-21	0.118	336.4	2.02E-21	0.112	336.6	3.00E-21	0.105	336.8	2.40E-21	0.099	337.0	3.07E-21	0.093
337.2	2.29E-21	0.087	337.4	2.46E-21	0.081	337.6	2.92E-21	0.074	337.8	8.10E-21	0.068	338.0	1.82E-20	0.062
338.2	3.10E-20	0.056	338.4	3.24E-20	0.050	338.6	4.79E-20	0.043	338.8	5.25E-20	0.037	339.0	5.85E-20	0.031
339.2	4.33E-20	0.025	339.4	4.20E-20	0.019	339.6	3.99E-20	0.012	339.8	3.11E-20	0.006	340.0	2.72E-20	0.000

Photolysis File = HCHONEWM

WL (nm)	Abs (cm^2)	QY	WL (nm)	Abs (cm^2)	QY	WL (nm)	Abs (cm^2)	QY	WL (nm)	Abs (cm^2)	QY	WL (nm)	Abs (cm^2)	QY
280.0	2.49E-20	0.350	280.5	1.42E-20	0.346	281.0	1.51E-20	0.341	281.5	1.32E-20	0.336	282.0	9.73E-21	0.332
282.5	6.76E-21	0.327	283.0	5.82E-21	0.323	283.5	9.10E-21	0.319	284.0	3.71E-20	0.314	284.5	4.81E-20	0.309
285.0	3.95E-20	0.305	285.5	2.87E-20	0.301	286.0	2.24E-20	0.296	286.5	1.74E-20	0.291	287.0	1.13E-20	0.287
287.5	1.10E-20	0.282	288.0	2.62E-20	0.278	288.5	4.00E-20	0.273	289.0	3.55E-20	0.269	289.5	2.12E-20	0.264
290.0	1.07E-20	0.260	290.5	1.35E-20	0.258	291.0	1.99E-20	0.256	291.5	1.56E-20	0.254	292.0	8.65E-21	0.252
292.5	5.90E-21	0.250	293.0	1.11E-20	0.248	293.5	6.26E-20	0.246	294.0	7.40E-20	0.244	294.5	5.36E-20	0.242
295.0	4.17E-20	0.240	295.5	3.51E-20	0.238	296.0	2.70E-20	0.236	296.5	1.75E-20	0.234	297.0	1.16E-20	0.232
297.5	1.51E-20	0.230	298.0	3.69E-20	0.228	298.5	4.40E-20	0.226	299.0	3.44E-20	0.224	299.5	2.02E-20	0.222
300.0	1.06E-20	0.220	300.4	7.01E-21	0.220	300.6	8.63E-21	0.221	300.8	1.47E-20	0.221	301.0	2.01E-20	0.221
301.2	2.17E-20	0.221	301.4	1.96E-20	0.221	301.6	1.54E-20	0.222	301.8	1.26E-20	0.222	302.0	1.03E-20	0.222
302.2	8.53E-21	0.222	302.4	7.13E-21	0.222	302.6	6.61E-21	0.223	302.8	1.44E-20	0.223	303.0	3.18E-20	0.223
303.2	3.81E-20	0.223	303.4	5.57E-20	0.223	303.6	6.91E-20	0.224	303.8	6.58E-20	0.224	304.0	6.96E-20	0.224
304.2	5.79E-20	0.224	304.4	5.24E-20	0.224	304.6	4.30E-20	0.225	304.8	3.28E-20	0.225	305.0	3.60E-20	0.225
305.2	5.12E-20	0.225	305.4	4.77E-20	0.225	305.6	4.43E-20	0.226	305.8	4.60E-20	0.226	306.0	4.01E-20	0.226
306.2	3.28E-20	0.226	306.4	2.66E-20	0.226	306.6	2.42E-20	0.227	306.8	1.95E-20	0.227	307.0	1.58E-20	0.227
307.2	1.37E-20	0.227	307.4	1.19E-20	0.227	307.6	1.01E-20	0.228	307.8	9.01E-21	0.228	308.0	8.84E-21	0.228
308.2	2.08E-20	0.228	308.4	2.39E-20	0.228	308.6	3.08E-20	0.229	308.8	3.39E-20	0.229	309.0	3.18E-20	0.229
309.2	3.06E-20	0.229	309.4	2.84E-20	0.229	309.6	2.46E-20	0.230	309.8	1.95E-20	0.230	310.0	1.57E-20	0.230
310.2	1.26E-20	0.233	310.4	9.26E-21	0.236	310.6	7.71E-21	0.239	310.8	6.05E-21	0.242	311.0	5.13E-21	0.245
311.2	4.82E-21	0.248	311.4	4.54E-21	0.251	311.6	6.81E-21	0.254	311.8	1.04E-20	0.257	312.0	1.43E-20	0.260
312.2	1.47E-20	0.263	312.4	1.35E-20	0.266	312.6	1.13E-20	0.269	312.8	9.86E-21	0.272	313.0	7.82E-21	0.275
313.2	6.48E-21	0.278	313.4	1.07E-20	0.281	313.6	2.39E-20	0.284	313.8	3.80E-20	0.287	314.0	5.76E-20	0.290
314.2	6.14E-20	0.293	314.4	7.45E-20	0.296	314.6	5.78E-20	0.299	314.8	5.59E-20	0.302	315.0	4.91E-20	0.305
315.2	4.37E-20	0.308	315.4	3.92E-20	0.311	315.6	2.89E-20	0.314	315.8	2.82E-20	0.317	316.0	2.10E-20	0.320
316.2	1.66E-20	0.323	316.4	2.05E-20	0.326	316.6	4.38E-20	0.329	316.8	5.86E-20	0.332	317.0	6.28E-20	0.335
317.2	5.07E-20	0.338	317.4	4.33E-20	0.341	317.6	4.17E-20	0.344	317.8	3.11E-20	0.347	318.0	2.64E-20	0.350
318.2	2.24E-20	0.353	318.4	1.70E-20	0.356	318.6	1.24E-20	0.359	318.8	1.11E-20	0.362	319.0	7.70E-21	0.365
319.2	6.36E-21	0.368	319.4	5.36E-21	0.371	319.6	4.79E-21	0.374	319.8	6.48E-21	0.377	320.0	1.48E-20	0.380
320.2	1.47E-20	0.386	320.4	1.36E-20	0.392	320.6	1.69E-20	0.399	320.8	1.32E-20	0.405	321.0	1.49E-20	0.411
321.2	1.17E-20	0.417	321.4	1.15E-20	0.423	321.6	9.64E-21	0.430	321.8	7.26E-21	0.436	322.0	5.94E-21	0.442
322.2	4.13E-21	0.448	322.4	3.36E-21	0.454	322.6	2.39E-21	0.461	322.8	2.01E-21	0.467	323.0	1.76E-21	0.473
323.2	2.82E-21	0.479	323.4	4.65E-21	0.485	323.6	7.00E-21	0.492	323.8	7.80E-21	0.498	324.0	7.87E-21	0.504
324.2	6.59E-21	0.510	324.4	5.60E-21	0.516	324.6	4.66E-21	0.523	324.8	4.21E-21	0.529	325.0	7.77E-21	0.535
325.2	2.15E-20	0.541	325.4	3.75E-20	0.547	325.6	4.10E-20	0.554	325.8	6.47E-20	0.560	326.0	7.59E-20	0.566
326.2	6.51E-20	0.572	326.4	5.53E-20	0.578	326.6	5.76E-20	0.585	326.8	4.43E-20	0.591	327.0	3.44E-20	0.597
327.2	3.22E-20	0.603	327.4	2.13E-20	0.609	327.6	1.91E-20	0.616	327.8	1.42E-20	0.622	328.0	9.15E-21	0.628
328.2	6.79E-21	0.634	328.4	4.99E-21	0.640	328.6	4.77E-21	0.647	328.8	1.75E-20	0.653	329.0	3.27E-20	0.659
329.2	3.99E-20	0.665	329.4	5.13E-20	0.671	329.6	4.00E-20	0.678	329.8	3.61E-20	0.684	330.0	3.38E-20	0.690
330.2	3.08E-20	0.694	330.4	2.16E-20	0.699	330.6	2.09E-20	0.703	330.8	1.41E-20	0.708	331.0	9.95E-21	0.712
331.2	7.76E-21	0.717	331.4	6.16E-21	0.721	331.6	4.06E-21	0.726	331.8	3.03E-21	0.730	332.0	2.41E-21	0.735
332.2	1.74E-21	0.739	332.4	1.33E-21	0.744	332.6	2.70E-21	0.748	332.8	1.65E-21	0.753	333.0	1.17E-21	0.757
333.2	9.84E-22	0.762	333.4	8.52E-22	0.766	333.6	6.32E-22	0.771	333.8	5.21E-22	0.775	334.0	1.46E-21	0.780
334.2	1.80E-21	0.784	334.4	1.43E-21	0.789	334.6	1.03E-21	0.793	334.8	7.19E-22	0.798	335.0	4.84E-22	0.802
335.2	2.73E-22	0.798	335.4	1.34E-22	0.794	335.6	0.00E+00	0.790	335.8	1.25E-22	0.786	336.0	4.47E-22	0.782
336.2	1.23E-21	0.778	336.4	2.02E-21	0.773	336.6	3.00E-21	0.769	336.8	2.40E-21	0.764	337.0	3.07E-21	0.759
337.2	2.29E-21	0.754	337.4	2.46E-21	0.749	337.6	2.92E-21	0.745	337.8	8.10E-21	0.740	338.0	1.82E-20	0.734
338.2	3.10E-20	0.729	338.4	3.24E-20	0.724	338.6	4.79E-20	0.719	338.8	5.25E-20	0.714	339.0	5.85E-20	0.709
339.2	4.33E-20	0.703	339.4	4.20E-20	0.698	339.6	3.99E-20	0.693	339.8	3.11E-20	0.687	340.0	2.72E-20	0.682
340.2	1.99E-20	0.676	340.4	1.76E-20	0.671	340.6	1.39E-20	0.666	340.8	1.01E-20	0.660	341.0	6.57E-21	0.655
341.2	4.83E-21	0.649	341.4	3.47E-21	0.643	341.6	2.23E-21	0.638	341.8	1.55E-21	0.632	342.0	3.70E-21	0.627
342.2	4.64E-21	0.621	342.4	1.08E-20	0.616	342.6	1.14E-20	0.610	342.8	1.79E-20	0.604	343.0	2.33E-20	0.599

Table 3. (continued)

WL (nm)	Abs (cm^2)	QY	WL (nm)	Abs (cm^2)	QY	WL (nm)	Abs (cm^2)	QY	WL (nm)	Abs (cm^2)	QY	WL (nm)	Abs (cm^2)	QY
Photolysis File = HCHONEWM (continued)														
343.2	1.72E-20	0.593	343.4	1.55E-20	0.588	343.6	1.46E-20	0.582	343.8	1.38E-20	0.576	344.0	1.00E-20	0.571
344.2	8.26E-21	0.565	344.4	6.32E-21	0.559	344.6	4.28E-21	0.554	344.8	3.22E-21	0.548	345.0	2.54E-21	0.542
345.2	1.60E-21	0.537	345.4	1.15E-21	0.531	345.6	8.90E-22	0.525	345.8	6.50E-22	0.520	346.0	5.09E-22	0.514
346.2	5.15E-22	0.508	346.4	3.45E-22	0.503	346.6	3.18E-22	0.497	346.8	3.56E-22	0.491	347.0	3.24E-22	0.485
347.2	3.34E-22	0.480	347.4	2.88E-22	0.474	347.6	2.84E-22	0.468	347.8	9.37E-22	0.463	348.0	9.70E-22	0.457
348.2	7.60E-22	0.451	348.4	6.24E-22	0.446	348.6	4.99E-22	0.440	348.8	4.08E-22	0.434	349.0	3.39E-22	0.428
349.2	1.64E-22	0.423	349.4	1.49E-22	0.417	349.6	8.30E-23	0.411	349.8	2.52E-23	0.406	350.0	2.57E-23	0.400
350.2	0.00E+00	0.394	350.4	5.16E-23	0.389	350.6	0.00E+00	0.383	350.8	2.16E-23	0.377	351.0	7.07E-23	0.371
351.2	3.45E-23	0.366	351.4	1.97E-22	0.360	351.6	4.80E-22	0.354	351.8	3.13E-21	0.349	352.0	6.41E-21	0.343
352.2	8.38E-21	0.337	352.4	1.55E-20	0.331	352.6	1.86E-20	0.326	352.8	1.94E-20	0.320	353.0	2.78E-20	0.314
353.2	1.96E-20	0.309	353.4	1.67E-20	0.303	353.6	1.75E-20	0.297	353.8	1.63E-20	0.291	354.0	1.36E-20	0.286
354.2	1.07E-20	0.280	354.4	9.82E-21	0.274	354.6	8.66E-21	0.269	354.8	6.44E-21	0.263	355.0	4.84E-21	0.257
355.2	3.49E-21	0.251	355.4	2.41E-21	0.246	355.6	1.74E-21	0.240	355.8	1.11E-21	0.234	356.0	7.37E-22	0.229
356.2	4.17E-22	0.223	356.4	1.95E-22	0.217	356.6	1.50E-22	0.211	356.8	8.14E-23	0.206	357.0	0.00E+00	0.200

Table 4. List of Model Species Added to the SAPRC-91 Mechanism used to Represent the Reactive Products of Isoprene in the Preliminary Detailed Isoprene Mechanism.

Name	Description
Isoprene Product Species	
MVK	Methylvinyl ketone
METHACRO	Methacrolein
MEFURAN	3-Methyl furan
ISOPROD	C_5 Methyl- and hydroxymethyl substituted acroleins assumed to be formed in the OH reaction following O_2 addition to the other allylic resonance form of the OH - isoprene adduct, and 1,5-H shift isomerization of the alkoxy radical(s) subsequently formed. Also used to represent uncharacterized products in the O^3P reaction.
Secondary Product Species	
HOACET	Hydroxyacetone
HOCCHO	Glycolaldehyde
MA-PAN	PAN analogue formed from methacrolein
AC-PAN	PAN analogue formed from acrolein and MVK
HO-PAN	PAN analogue formed from glycolaldehyde
IP-PAN	PAN analogue formed from reactions of ISOPROD
HET-UNKN	Photoreactive product(s) formed from furans (see Carter et al., 19??)

Acyl Peroxy Radicals (Listed in order of their corresponding PAN analogue, above.)

MA-RCO3.	AC-RCO3.	HOCCO-O2.	IP-RCO3.

Various Excited "Criegee" biradicals formed in the reaction of O_3 with Isoprene and its Products. (The names give an indication of the structure.)

(HCHO2)	(C:CC(C)O2)	(C:C(C)CHO2)	(C2(.)(O2.)CHO)
(C-CO-CHO2)	(HOCCHO2)	(HCOCHO2)	(HOC2.O2.CH3)

Table 5. Listing of Reactions in the Preliminary Detailed Mechanism for Isoprene.

Rxn. Label	Kinetic Parameters [a]				Reactions [b]
	k(300)	A	Ea	B	
Isoprene					
ISOH	1.46E+05	3.73E+04	-0.81	-1.00	ISOP + HO. = #.58 HCHO + #.34 MVK + #.24 METHACRO + #.05 MEFURAN + #.31 ISOPROD + #.09 R2O2. + #.94 RO2-R. + #.06 RO2-N. + #1.09 RO2.
ISO3	2.20E-02	1.81E+01	4.00	-1.00	ISOP + O3 = #.5 HCHO + #.25 "METHACRO + MVK" + #.5 (HCHO2) + #.25 "(C:CC(C)O2) + (C:C(C)CHO2)"
ZIS1	6.00E+01	(No T Dependence)			(C:CC(C)O2) = #.42 "HO. + MA-RCO3. + HCHO + R2O2. + RCO3. + RO2." + #.58 "ISOPROD + #-1 -C"
ZIS2	6.00E+01	(No T Dependence)			(C:C(C)CHO2) = #.42 "HO2. + CO + HCHO + HOCCO-O2. + RCO3." + #.58 "ISOPROD + #-1 -C"
ISOA	8.81E+04	8.81E+04	0.00	-1.00	ISOP + O = #.93 ISOPROD + #.07 "AC-RCO3. + RCO3. + HCHO + RO2-R. + RO2."
ISN3	1.62E+03	3.74E+04	1.87	-1.00	ISOP + NO3 = #.4 HCHO + #.3 MVK + #.1 METHACRO + #.4 ISOPROD + #.8 NO2 + #.95 R2O2. + #.2 "RO2-R. + RNO3" + #1.15 RO2.
Methacrolein [c]					
MA1	4.89E+04	2.73E+04	-0.35	-1.00	METHACRO + HO. = #.5 "MA-RCO3. + RCO3." + #.42 "HOACET + CO" + #.08 "HCHO + MGLY" + #.5 "RO2-R. + RO2."
MA2	1.84E-03	8.09E+00	5.00	-1.00	METHACRO + O3 = #.5 "(HCHO2) + HCHO + MGLY + (C2(.)(O2.)CHO)"
Z1	6.00E+01	(No T Dependence)			(HCHO2) = #.37 O3OL-SB + #.12 "HO2. + CO + HO." + #.88 -C
MAZ1	6.00E+01	(No T Dependence)			(C2(.)(O2.)CHO) = #.435 "O3OL-SB + #3 -C" + #.565 "HO. + HCHO + #2 CO + RO2-R. + RO2."
MA3	(Phot. Set = ACROLEIN)				METHACRO + HV + #2.06E-3 = HO2. + CO + HCHO + CCO-O2. + RCO3.
MA5	4.26E+00	2.11E+03	3.70	-1.00	METHACRO + NO3 = MA-RCO3. + RCO3. + HNO3
MAP1	(Same k as Reaction B2)				MA-RCO3. + NO = NO2 + CO2 + HCHO + CCO-O2. + RCO3.
MAP2	8.73E+03	8.73E+03	0.00	-4.60	MA-RCO3. + NO2 = MA-PAN
MAP3	(Same k as Reaction B6)				MA-RCO3. + HO2. = -OOH + #2 "HCHO + CO2"
MAP4	(Same k as Reaction B9)				MA-RCO3. + RO2. = RO2. + #.5 HO2. + #2 "HCHO + CO2"
MAP5	(Same k as Reaction B10)				MA-RCO3. + RCO3. = RCO3. + HO2. + #2 "HCHO + CO2"
MAP6	4.07E-02	9.60E+18	27.97	0.00	MA-PAN = MA-RCO3. + NO2 + RCO3.
Methylvinyl Ketone [c]					
MV1	2.74E+04	6.08E+03	-0.90	-1.00	MVK + HO. = #.7 "HOCCHO + R2O2. + CCO-O2. + RCO3." + #.3 "HCHO + MGLY + RO2-R." + RO2.
MV2	7.67E-03	6.29E+00	4.00	-1.00	MVK + O3 = #.5 "(HCHO2) + HCHO + MGLY + (C-CO-CHO2)"
MVZ1	6.00E+01	(No T Dependence)			(C-CO-CHO2) = #.74 "O3OL-SB + #3 -C" + #.26 "HO. + HCHO + #2 CO + RO2-R. + RO2."
MV4	(Phot. Set = ACROLEIN)				MVK + HV + #2.1E-3 = HCHO + RO2-R. + RO2. + AC-RCO3. + RCO3.
ACP1	(Same k as Reaction B2)				AC-RCO3. + NO = NO2 + CO2 + HCHO + CO + HO2.
ACP2	8.73E+03	8.73E+03	0.00	-4.60	AC-RCO3. + NO2 = AC-PAN
ACP3	(Same k as Reaction B6)				AC-RCO3. + HO2. = -OOH + HCHO + CO + CO2
ACP4	(Same k as Reaction B9)				AC-RCO3. + RO2. = RO2. + #.5 HO2. + HCHO + CO + CO2
ACP5	(Same k as Reaction B10)				AC-RCO3. + RCO3. = RCO3. + HO2. + HCHO + CO + CO2
ACP6	4.07E-02	9.60E+18	27.97	0.00	AC-PAN = AC-RCO3. + NO2 + RCO3.
Hydroxyacetone					
IP18	3.38E+03	3.38E+03	0.00	-1.00	HOACET + HO. = MGLY + HO2.
IP19	(Phot. Set = ACETONE)				HOACET + HV = CCO-O2. + RCO3. + HCHO + HO2.
Glycolaldehyde					
IP20	1.45E+04	1.45E+04	0.00	-1.00	HOCCHO + HO. = #.8 "HOCCO-O2. + H2O + RCO3." + #.2 "GLY + HO2."
IP21	(Phot. Set = CCHOR)				HOCCHO + HV = CO + HCHO + #2 HO2.
IP22	4.17E+00	2.05E+03	3.70	-1.00	HOCCHO + NO3 = HNO3 + HOCCO-O2. + RCO3.
IP23	(Same k as Reaction B2)				HOCCO-O2. + NO = CO2 + NO2 + HCHO + HO2.
IP24	(Same k as Reaction B4)				HOCCO-O2. + NO2 = HO-PAN
IP25	(Same k as Reaction B6)				HOCCO-O2. + HO2. = -OOH + CO2 + HCHO
IP26	(Same k as Reaction B9)				HOCCO-O2. + RO2. = RO2. + #.5 HO2. + CO2 + HCHO
IP27	(Same k as Reaction B10)				HOCCO-O2. + RCO3. = RCO3. + HO2. + CO2 + HCHO
IP28	(Same k as Reaction C18)				HO-PAN = HOCCO-O2. + NO2 + RCO3.
Methyl furan					
K4	1.38E+05	1.38E+05	0.00	-1.00	HO. + MEFURAN = #.245 "R2O2. + RO2." + HO2. + #.475 HET-UNKN
K5	2.05E+04	2.05E+04	0.00	-1.00	NO3 + MEFURAN = HO2. + HNO3
K3	(Phot. Set = ACROLEIN)				HET-UNKN + HV = #2 HO2.
C_5 Methyl, Hydroxymethyl Acroleins [d]					
IPOH	5.87E+04	5.87E+04	0.00	-1.00	ISOPROD + HO. = #.4 "IP-RCO3. + RCO3." + #.2 MEK + #.2 GLY + #.2 HOACET + #.1 HOCCHO + #.1 ACET + #.1 "RCHO + -C" + #.3 CO + #.6 "RO2-R. + RO2."
IPP1	(Same k as Reaction B2)				IP-RCO3. + NO = NO2 + CO2 + #.5 "CO + HO2. + CCO-O2. + RCO3. + HOCCHO + HOACET"

Table 5 (continued)

Rxn. Label	Kinetic Parameters [a]				Reactions [b]
	k(300)	A	Ea	B	
IPP2	8.73E+03	8.73E+03	0.00	-4.60	IP-RCO3. + NO2 = IP-PAN
IPP3	(Same k as Reaction B6)				IP-RCO3. + HO2. = -OOH + #1.5 CO2 + #.5 "CO + HCHO + HOCCHO + HOACET"
IPP4	(Same k as Reaction B9)				IP-RCO3. + RO2. = RO2. + #.5 HO2. + #.5 "CO + HCHO + HOCCHO + HOACET"
IPP5	(Same k as Reaction B10)				IP-RCO3. + RCO3. = RCO3. + HO2. + #.5 "CO + HCHO + HOCCHO + HOACET"
IPP6	4.07E-02	9.60E+18	27.97	0.00	IP-PAN = IP-RCO3. + NO2 + RCO3.
IPO3	9.32E-02	8.07E+00	2.66	-1.00	ISOPROD + O3 = #.25 "HOACET + HOCCHO + ACET + GLY + (HOCCHO2) + (HCOCHO2) + (C2(.)(O2.)CHO) + (HOC2.O2.CH3)"
ZAC	6.00E+01	(No T Dependence)			(HCOCHO2) = #.435 "O3OL-SB + #2 -C" + #.565 "CO2 + #2 HO2. + CO"
ZIP1	6.00E+01	(No T Dependence)			(HOCCHO2) = #.7 "O3OL-SB + #2 -C" + #.3 HCHO + #.15 CO2 + #.45 HO2. + #.15 "CO + HO."
ZIP2	6.00E+01	(No T Dependence)			(HOC2.O2.CH3) = #.8 "MEK + #-1 -C" + #.2 "HO. + MGLY + HO2."
IPHV	(Phot. Set = ACROLEIN)				ISOPROD + HV + #2.06E-3 = HCHO + #1.5 HO2. + #.5 "ACET + CO + GLY + RCO3." + #.3 HOCCO-O2. + #.2 CCO-O2.
IPN3	4.26E+00	2.11E+03	3.70	-1.00	ISOPROD + NO3 = IP-RCO3. + RCO3. + HNO3

[a] Except as noted, expression for rate constant is k = A $e^{Ea/RT}$ $(T/300)^B$. Rate constants and A factor are in ppm, min units. Units of Ea is kcal $mole^{-1}$. "Phot Set" means this is a photolysis reaction, with the absorption coefficients and quantum yields given in Carter (1990) or in Table ?.

[b] Format of reaction listing same as used in documentation of the detailed mechanism (Carter 1990).

[c] Overall photolysis quantum yield and radical yield in ozone reaction adjusted to yield best fit of model simulations to results of methacrolein - NO_x - air or methylvinyl ketone - NO_x - air chamber experiments.

[d] Overall photolysis quantum yield and radical yield in ozone reaction assumed to be same as for methacrolein. Rate constant for ozone reaction adjusted to give best fit to model simulations of SAPRC isoprene runs.

represented by a single model species, with product yields being derived based on the distribution of isomers expected to be formed.) The mechanisms for methacrolein and methylvinyl ketone have been adjusted to simulate results of environmental chamber experiments employing those compounds, and the mechanisms for the C_5 hydroxy-substituted acroleins have been adjusted in part to simulate isoprene - NO_x - air runs. The species added to the SAPRC-91 mechanism to represent isoprene and its products are given in Table 4 and 5, respectively. This mechanism performs significantly better than the SAPRC-90 mechanism (e. g., see Carter and Lurmann, 1991) in simulating the results of the isoprene experiments (Carter, unpublished results).

This mechanism is preliminary and still under development, and a more detailed documentation of it is beyond the scope of this report. (In many respects it is similar to the recently published mechanism of Paulson and Seinfeld [1992].) It is presented here to illustrate the degree to which the results of these experiments are consistent with our current and most detailed estimates for the atmospheric reactions of isoprene and its major products. Note that while this mechanism was adjusted to fit isoprene and isoprene product - NO_x - air chamber experiments, the results of these reactivity experiments were not used in its development, so they provide an independent test of this mechanism.

Carbon Bond Mechanism

The Carbon Bond IV mechanism used in the calculations discussed here is based on that documented by Gery et al (1988), but modified as recommended by the EPA (Dodge, personal communication, 1991) The species in this mechanism are the same as given by Gery et. al (1988), and reactions of this version of the mechanism are listed in Table 6. The modifications relative to the documented (Gery et al., 1988) mechanism include adding the XO2 + HO2 reaction as recommended by Dodge (1990), and updating the kinetics for PAN formation and formaldehyde photolysis. Absorption cross section and quantum yield data for this mechanism were supplied by Gery (personal communication), and are listed on Table 7.

Like the unadjusted SAPRC-91 mechanism (Appendix A), the unadjusted Carbon Bond mechanism also significantly underpredicted the rate of ozone formation in the base case experiment. Thus, it had to be adjusted before it could be used to simulate reactivities measured in these experiments. The need for such an adjustment is not surprising in this case, since this mechanism was not designed to simulate aromatic chemistry with a blacklight light source. In this case, the adjustment consisted of increasing the photolysis rates of the two model species used to represent photoreactive aromatic fragmentation products (MGLY and OPEN) by a factor of two.

The Carbon Bond IV mechanism includes a separate representation for the reaction of isoprene, though like the SAPRC-90 mechanism it does not use separate model species to represent the reactions of its products. However, unlike SAPRC-90 which uses a generalized procedure which is applied to all the alkenes to represent the products, the Carbon Bond isoprene mechanism uses a mix of species already in the model to represent the type of reactions the Carbon Bond developers felt the isoprene products might undergo, with adjustments being made to fit results of isoprene-NO_x outdoor chamber experiments (Gery et. al. 1988). For example, ethene is represented among the mix of species isoprene is represented to form, to account for the fact that isoprene is expected to form products which react with ozone.

Chamber Effects Model

The testing of a chemical mechanism against environmental chamber data requires including in the model appropriate representations for chamber-dependent effects such as wall reactions and characteristics of the light source used during the experiments. The methods used to represent them in this study are based on those discussed in detail by Carter and Lurmann (1990, 1991), adapted

Table 6. Listing of The Carbon Bond IV Mechanism as used to Simulate Results of Isoprene Reactivity Experiments.

Rxn. Label	Kinetic Parameters [a] k(300)	A	Ea	B	Reactions [b]
					BASE CASE REACTIONS [c]
1	(Phot. Set = NO2CB)				NO2 + HV = NO + O
2	4.32E+06	8.61E+04	-2.33	0.00	O = O3
3	2.66E+01	2.56E+03	2.72	0.00	O3 + NO = NO2
4	1.37E+04	(No T Dependence)			O + NO2 = NO
5	2.31E+03	2.34E+02	-1.37	0.00	O + NO2 = NO3
6	2.44E+03	3.28E+02	-1.20	0.00	O + NO = NO2
7	4.73E-02	1.67E+02	4.87	0.00	NO2 + O3 = NO3
8	(Phot. Set = O3O3PCB)				O3 + HV = O
9	(Phot. Set = O3O1DCB)				O3 + HV = O1D
10	4.25E+05	1.16E+05	-0.78	0.00	O1D = O
11	3.26E+00	(No T Dependence)			O1D + H2O = #2 OH
12	1.00E+02	2.29E+03	1.87	0.00	O3 + OH = HO2
13	3.00E+00	2.07E+01	1.15	0.00	O3 + HO2 = OH
14	(Phot. Set = NO3CBEST)				NO3 + HV = #.89 NO2 + #.89 O + #.11 NO
15	4.42E+04	1.92E+04	-0.50	0.00	NO3 + NO = #2 NO2
16	5.90E-01	3.56E+01	2.44	0.00	NO3 + NO2 = NO + NO2
17	1.85E+03	7.89E+02	-0.51	0.00	NO3 + NO2 = N2O5
18	1.90E-06	(No T Dependence)			N2O5 + H2O = #2 HNO3
19	2.78E+00	1.65E+16	21.65	0.00	N2O5 = NO3 + NO2
20	1.54E-04	2.63E-05	-1.05	0.00	NO + NO = #2 NO2
21	1.60E-11	(No T Dependence)			NO + NO2 + H2O = #2 HONO
22	9.80E+03	6.67E+02	-1.60	0.00	NO + OH = HONO
23	(Phot. Set = HONOCB)				HONO + HV = NO + OH
25	1.50E-05	(No T Dependence)			HONO + HONO = NO + NO2
26	1.68E+04	1.56E+03	-1.42	0.00	NO2 + OH = HNO3
27	2.18E+02	7.77E+00	-1.99	0.00	OH + HNO3 = NO3
28	1.23E+04	5.51E+03	-0.48	0.00	HO2 + NO = OH + NO2
29	2.02E+03	1.67E+02	-1.49	0.00	HO2 + NO2 = PNA
30	5.11E+00	2.29E+15	20.11	0.00	PNA = HO2 + NO2
31	6.83E+03	1.92E+03	-0.76	0.00	OH + PNA = NO2
32	4.14E+03	8.97E+01	-2.29	0.00	HO2 + HO2 = H2O2
33	2.18E-01	8.76E-10	-11.53	0.00	HO2 + HO2 + H2O = H2O2
34	(Phot. Set = H2O2CB)				H2O2 + HV = #2 OH
35	2.52E+03	4.70E+03	0.37	0.00	OH + H2O2 = HO2
36	3.22E+02	(No T Dependence)			OH + CO = HO2
37	1.50E+04	(No T Dependence)			HCHO + OH = HO2 + CO
38	(Phot. Set = HCHORMCB)				HCHO + HV = #2 HO2 + CO
39	(Phot. Set = HCHOSMCB)				HCHO + HV = CO
40	2.37E+02	4.15E+04	3.08	0.00	HCHO + O = OH + HO2 + CO
41	9.30E-01	(No T Dependence)			HCHO + NO3 = HNO3 + HO2 + CO
42	6.36E+02	1.70E+04	1.96	0.00	ALD2 + O = C2O3 + OH
43	2.40E+04	1.04E+04	-0.50	0.00	ALD2 + OH = C2O3
44	3.70E+00	(No T Dependence)			ALD2 + NO3 = C2O3 + HNO3
45	(Phot. Set = ALD2RCB)				ALD2 + HV = HCHO + #2 HO2 + CO + XO2
46	2.83E+04	5.15E+04	0.36	0.00	C2O3 + NO = HCHO + NO2 + HO2 + XO2
47	1.36E+04	3.84E+03	-0.76	0.00	C2O3 + NO2 = PAN
48	3.44E-02	1.20E+18	26.83	0.00	PAN = C2O3 + NO2
49	3.70E+03	(No T Dependence)			C2O3 + C2O3 = #2 HCHO + #2 XO2 + #2 HO2
50	9.60E+03	(No T Dependence)			C2O3 + HO2 = #.79 HCHO + #.79 XO2 + #.79 HO2 + #.79 OH
51	2.10E+01	6.28E+03	3.40	0.00	OH = HCHO + XO2 + HO2
52	1.20E+03	(No T Dependence)			PAR + OH = #.87 XO2 + #.130 XO2N + #.11 HO2 + #.11 ALD2 + #-0.11 PAR + #.76 ROR
53	1.37E+05	5.23E+16	15.90	0.00	ROR = #.96 XO2 + #1.1 ALD2 + #.94 HO2 + #-2.1 PAR + #.04 XO2N + #.02 ROR
54	9.54E+04	(No T Dependence)			ROR = HO2
55	2.20E+04	(No T Dependence)			ROR + NO2 =
56	5.92E+03	1.74E+04	0.64	0.00	O + OLE = #.63 ALD2 + #.38 HO2 + #.28 XO2 + #.30 CO + #.20 HCHO + #.02 XO2N + #.22 PAR + #.2 OH
57	4.20E+04	7.83E+03	-1.00	0.00	OH + OLE = HCHO + ALD2 + #-1.0 PAR + XO2 + HO2
58	1.80E-02	2.01E+01	4.18	0.00	O3 + OLE = #.5 ALD2 + #.740 HCHO + #.220 XO2 + #.10 OH + #.330 CO + #.44 HO2 + #-1.0 PAR
59	1.14E+01	(No T Dependence)			NO3 + OLE = #.91 XO2 + HCHO + #.09 XO2N + ALD2 + NO2 + #-1 PAR
60	1.08E+03	1.51E+04	1.57	0.00	O + ETH = HCHO + #1.7 HO2 + CO + #.7 XO2 + #.3 OH
61	1.19E+04	3.03E+03	-0.82	0.00	OH + ETH = XO2 + #1.56 HCHO + #.22 ALD2 + HO2
62	2.70E-03	1.75E+01	5.23	0.00	O3 + ETH = HCHO + #.42 CO + #.12 HO2
63	9.15E+03	3.13E+03	-0.64	0.00	TOL + OH = #.44 HO2 + #.08 XO2 + #.36 CRES + #.56 TO2
64	1.20E+04	(No T Dependence)			TO2 + NO = #.90 NO2 + #.90 HO2 + #.90 OPEN
65	2.50E+02	(No T Dependence)			TO2 = CRES + HO2
66	6.10E+04	(No T Dependence)			OH + CRES = #.40 CRO + #.60 XO2 + #.60 HO2 + #.30 OPEN
67	3.25E+04	(No T Dependence)			CRES + NO3 = CRO + HNO3
68	2.00E+04	(No T Dependence)			CRO + NO2 =
69	(Phot. Set = HCHORBCB)				OPEN + **#Fudge** + #9.04 + HV = C2O3 + HO2 + CO **(see note [d])**
70	4.40E+04	(No T Dependence)			OPEN + OH = XO2 + #2 CO + #2 HO2 + C2O3 + HCHO
71	1.50E-02	7.94E-02	0.99	0.00	OPEN + O3 = #.03 ALD2 + #.62 C2O3 + #.70 HCHO + #.03 XO2 + #.69 CO + #.08 OH + #.76 HO2 + #.20 MGLY
72	3.62E+04	2.46E+04	-0.23	0.00	OH + XYL = #.70 HO2 + #.50 XO2 + #.20 CRES + #.8 MGLY + #1.1 PAR +

Table 6 (continued)

Rxn. Label	Kinetic Parameters [a]				Reactions [b]
	k(300)	A	Ea	B	
					#.30 TO2
73	2.60E+04	(No T Dependence)			OH + MGLY = XO2 + C2O3
74	(Phot. Set = HCHORBCB)				MGLY + **#Fudge** + #9.64 + HV = C2O3 + HO2 + CO **(see note [d])**
79	1.20E+04	(No T Dependence)			XO2 + NO = NO2
80	1.00E+03	(No T Dependence)			XO2N + NO =
81	2.00E+03	2.63E+01	-2.58	0.00	XO2 + XO2 =
82	8.64E+03	1.13E+02	-2.58	0.00	XO2 + HO2 =
					ISOPRENE REACTIONS
75	2.70E+04	(No T Dependence)			O + ISOP = #.60 HO2 + #.8 ALD2 + #.55 OLE + #.5 XO2 + #.5 CO + #.450 ETH + #.9 PAR + #R-ISOP TEST_RCT
76	1.42E+05	(No T Dependence)			OH + ISOP = XO2 + HCHO + #.67 HO2 + #.13 XO2N + ETH + #.4 MGLY + #.2 C2O3 + #.2 ALD2 +#R-ISOP TEST_RCT
77	1.80E-02	(No T Dependence)			O3 + ISOP = HCHO + #.4 ALD2 + #.55 ETH + #.2 MGLY + #.1 PAR + #.060 CO + #.44 HO2 + #.1 OH + #R-ISOP TEST_RCT
78	4.70E+02	(No T Dependence)			NO3 + ISOP = XO2N + #R-ISOP TEST_RCT
					CHAMBER-DEPENDENT REACTIONS (Applicable for these ETC runs only)
O3W	3.70E-04	(No T Dependence)			O3 =
N25I	2.50E-03	(No T Dependence)			N2O5 = #2 NOX-WALL
N25S	5.00E+08	(No T Dependence)			N2O5 + H2O = #2 NOX-WALL
NO2W	1.40E-04	(No T Dependence)			NO2 = #.2 HONO + #.8 NOX-WALL
RSI	(Same k as Reaction 1)				HV + #2.E-5 = OH
ONO2	(Same k as Reaction 1)				HV + #1.1E-4 = NO2 + #-1 NOX-WALL
XSHC	2.50E+02	(No T Dependence)			OH = HO2

[a] Except as noted, expression for rate constant is $k = A\ e^{Ea/RT}\ (T/300)^{B}$. Rate constants and A factor are in ppm, min units. Units of Ea is kcal $mole^{-1}$. "Phot Set" means this is a photolysis reaction, with the absorption coefficients and quantum yields given in Table ?.

[b] Format of reaction listing same as used in documentation of the detailed mechanism (Carter 1990).

[c] Not all reactions in this listing are needed to simulate the experiments discussed here. The entire mechanism is given for completeness.

[d] The rates of these photolysis reactions were multiplied by a factor of two relative to the standard mechanism to simulate the base case experiments. "Fudge" is 1 for the standard mechanism, while "Fudge" = 2 was used for simulating these experiments.

Table 7. Absorption Cross Sections and Quantum Yields for Photolysis Reactions in the Carbon Bond IV Mechanism as Used to Simulate the Isoprene Reactivity Experiments.

WL (nm)	Abs (cm^2)	QY	WL (nm)	Abs (cm^2)	QY	WL (nm)	Abs (cm^2)	QY	WL (nm)	Abs (cm^2)	QY	WL (nm)	Abs (cm^2)	QY
Photolysis File = NO2CB														
280.0	5.54E-20	0.984	281.0	5.58E-20	0.984	282.0	5.36E-20	0.984	283.0	5.36E-20	0.984	284.0	6.25E-20	0.984
285.0	6.99E-20	0.984	286.0	7.29E-20	0.984	287.0	7.37E-20	0.984	288.0	7.66E-20	0.984	289.0	7.89E-20	0.984
290.0	8.18E-20	0.984	291.0	9.90E-20	0.984	292.0	9.37E-20	0.984	293.0	9.75E-20	0.984	294.0	9.48E-20	0.984
295.0	9.68E-20	0.984	296.0	9.30E-20	0.983	297.0	1.22E-19	0.982	298.0	1.17E-19	0.982	299.0	1.26E-19	0.981
300.0	1.17E-19	0.980	301.0	1.23E-19	0.980	302.0	1.39E-19	0.978	303.0	1.59E-19	0.978	304.0	1.60E-19	0.977
305.0	1.66E-19	0.976	306.0	1.58E-19	0.975	307.0	1.63E-19	0.974	308.0	1.62E-19	0.973	309.0	1.84E-19	0.973
310.0	1.76E-19	0.972	311.0	1.88E-19	0.971	312.0	1.96E-19	0.970	313.0	2.04E-19	0.970	314.0	1.94E-19	0.969
315.0	2.25E-19	0.968	316.0	2.13E-19	0.967	317.0	2.33E-19	0.966	318.0	2.48E-19	0.966	319.0	2.31E-19	0.965
320.0	2.54E-19	0.964	321.0	2.65E-19	0.963	322.0	2.65E-19	0.962	323.0	2.77E-19	0.962	324.0	2.67E-19	0.961
325.0	2.79E-19	0.960	326.0	2.88E-19	0.959	327.0	2.91E-19	0.958	328.0	3.08E-19	0.958	329.0	3.00E-19	0.957
330.0	2.99E-19	0.956	331.0	3.05E-19	0.955	332.0	3.01E-19	0.954	333.0	3.73E-19	0.954	334.0	2.98E-19	0.953
335.0	3.45E-19	0.952	336.0	3.51E-19	0.951	337.0	3.46E-19	0.950	338.0	3.48E-19	0.950	339.0	3.99E-19	0.949
340.0	3.88E-19	0.948	341.0	4.17E-19	0.947	342.0	3.83E-19	0.946	343.0	3.54E-19	0.946	344.0	4.02E-19	0.945
345.0	4.07E-19	0.944	346.0	4.29E-19	0.943	347.0	4.28E-19	0.942	348.0	4.82E-19	0.942	349.0	4.61E-19	0.941
350.0	4.10E-19	0.940	351.0	4.52E-19	0.939	352.0	4.44E-19	0.938	353.0	3.99E-19	0.938	354.0	5.04E-19	0.937
355.0	5.13E-19	0.936	356.0	4.60E-19	0.935	357.0	5.58E-19	0.934	358.0	5.04E-19	0.934	359.0	4.55E-19	0.933
360.0	4.51E-19	0.932	361.0	5.39E-19	0.931	362.0	5.04E-19	0.930	363.0	5.12E-19	0.930	364.0	4.87E-19	0.929
365.0	5.78E-19	0.928	366.0	5.40E-19	0.912	367.0	5.19E-19	0.896	368.0	5.34E-19	0.881	369.0	5.18E-19	0.865
370.0	5.42E-19	0.849	371.0	5.21E-19	0.833	372.0	5.98E-19	0.817	373.0	5.50E-19	0.802	374.0	5.21E-19	0.786
375.0	5.35E-19	0.770	376.0	6.24E-19	0.780	377.0	5.67E-19	0.920	378.0	5.17E-19	0.820	379.0	5.47E-19	0.870
380.0	5.99E-19	0.900	381.0	5.66E-19	0.810	382.0	5.64E-19	0.700	383.0	5.37E-19	0.680	384.0	5.97E-19	0.700
385.0	5.94E-19	0.770	386.0	5.32E-19	0.840	387.0	5.60E-19	0.750	388.0	5.98E-19	0.810	389.0	6.02E-19	0.780
390.0	6.00E-19	0.800	391.0	5.83E-19	0.880	392.0	6.05E-19	0.840	393.0	5.45E-19	0.900	394.0	5.54E-19	0.900
395.0	5.89E-19	0.840	396.0	6.15E-19	0.830	397.0	5.67E-19	0.820	398.0	6.41E-19	0.770	399.0	5.60E-19	0.780

Table 7 (continued)

Photolysis File = NO2CB (continued)

WL (nm)	Abs (cm^2)	QY	WL (nm)	Abs (cm^2)	QY	WL (nm)	Abs (cm^2)	QY	WL (nm)	Abs (cm^2)	QY	WL (nm)	Abs (cm^2)	QY
400.0	6.76E-19	0.680	401.0	6.53E-19	0.650	402.0	5.71E-19	0.620	403.0	5.10E-19	0.570	404.0	6.07E-19	0.420
405.0	6.32E-19	0.320	406.0	5.39E-19	0.330	407.0	4.73E-19	0.250	408.0	6.26E-19	0.200	409.0	5.90E-19	0.190
410.0	5.77E-19	0.150	411.0	5.88E-19	0.100	412.0	5.36E-19	0.090	413.0	7.00E-19	0.080	414.0	5.94E-19	0.080
415.0	6.04E-19	0.070	416.0	4.85E-19	0.060	417.0	5.31E-19	0.050	418.0	5.52E-19	0.040	419.0	5.28E-19	0.030
420.0	5.77E-19	0.020	421.0	5.80E-19	0.000									

Photolysis File = O3O1DCB

WL (nm)	Abs (cm^2)	QY	WL (nm)	Abs (cm^2)	QY	WL (nm)	Abs (cm^2)	QY	WL (nm)	Abs (cm^2)	QY	WL (nm)	Abs (cm^2)	QY
280.0	3.97E-18	0.900	281.0	3.60E-18	0.900	282.0	3.24E-18	0.900	283.0	3.01E-18	0.900	284.0	2.73E-18	0.900
285.0	2.44E-18	0.900	286.0	2.21E-18	0.900	287.0	2.01E-18	0.900	288.0	1.76E-18	0.900	289.0	1.58E-18	0.900
290.0	1.41E-18	0.900	291.0	1.26E-18	0.900	292.0	1.10E-18	0.900	293.0	9.89E-19	0.900	294.0	8.62E-19	0.900
295.0	7.67E-19	0.900	296.0	6.64E-19	0.900	297.0	5.88E-19	0.900	298.0	5.10E-19	0.900	299.0	4.52E-19	0.900
300.0	3.92E-19	0.900	301.0	3.44E-19	0.900	302.0	3.03E-19	0.900	303.0	2.63E-19	0.900	304.0	2.35E-19	0.900
305.0	2.02E-19	0.884	306.0	1.80E-19	0.848	307.0	1.56E-19	0.800	308.0	1.36E-19	0.740	309.0	1.23E-19	0.660
310.0	1.03E-19	0.560	311.0	9.27E-20	0.450	312.0	8.00E-20	0.340	313.0	6.92E-20	0.250	314.0	6.29E-20	0.180
315.0	5.22E-20	0.120	316.0	4.78E-20	0.080	317.0	4.04E-20	0.050	318.0	3.72E-20	0.020	319.0	2.91E-20	0.000

Photolysis File = O3O3PCB

WL (nm)	Abs (cm^2)	QY	WL (nm)	Abs (cm^2)	QY	WL (nm)	Abs (cm^2)	QY	WL (nm)	Abs (cm^2)	QY	WL (nm)	Abs (cm^2)	QY
280.0	3.97E-18	0.100	282.0	3.24E-18	0.100	284.0	2.73E-18	0.100	286.0	2.21E-18	0.100	288.0	1.76E-18	0.100
290.0	1.41E-18	0.100	292.0	1.10E-18	0.100	294.0	8.62E-19	0.100	296.0	6.64E-19	0.100	298.0	5.10E-19	0.100
300.0	3.92E-19	0.100	302.0	3.03E-19	0.100	304.0	2.35E-19	0.100	306.0	1.80E-19	0.152	308.0	1.36E-19	0.260
310.0	1.03E-19	0.440	312.0	8.00E-20	0.660	314.0	6.29E-20	0.820	316.0	4.78E-20	0.920	318.0	3.72E-20	0.980
320.0	2.99E-20	1.000	322.0	2.17E-20	1.000	324.0	1.29E-20	1.000	326.0	1.16E-20	1.000	328.0	1.11E-20	1.000
330.0	5.76E-21	1.000	332.0	4.58E-21	1.000	334.0	5.02E-21	1.000	336.0	2.16E-21	1.000	338.0	2.29E-21	1.000
340.0	1.21E-21	1.000	342.0	9.60E-22	1.000	344.0	7.12E-22	1.000	346.0	5.24E-22	1.000	348.0	3.95E-22	1.000
350.0	2.66E-22	1.000	352.0	2.03E-22	1.000	354.0	1.40E-22	1.000	356.0	9.80E-23	1.000	358.0	7.70E-23	1.000
360.0	5.50E-23	1.000	362.0	0.00E+00	1.000	418.0	0.00E+00	1.000	420.0	4.00E-23	1.000	422.0	5.00E-23	1.000
424.0	6.00E-23	1.000	426.0	7.00E-23	1.000	428.0	7.00E-23	1.000	430.0	8.00E-23	1.000	432.0	9.00E-23	1.000
434.0	1.00E-22	1.000	436.0	1.10E-22	1.000	438.0	1.20E-22	1.000	440.0	1.30E-22	1.000	442.0	1.50E-22	1.000
444.0	1.70E-22	1.000	446.0	1.90E-22	1.000	448.0	2.20E-22	1.000	450.0	2.40E-22	1.000	452.0	2.60E-22	1.000
454.0	2.90E-22	1.000	456.0	3.10E-22	1.000	458.0	3.30E-22	1.000	460.0	3.60E-22	1.000	462.0	3.90E-22	1.000
464.0	4.30E-22	1.000	466.0	4.60E-22	1.000	468.0	5.00E-22	1.000	470.0	5.30E-22	1.000	472.0	5.70E-22	1.000
474.0	6.00E-22	1.000	476.0	6.40E-22	1.000	478.0	6.80E-22	1.000	480.0	7.10E-22	1.000	482.0	7.60E-22	1.000
484.0	8.10E-22	1.000	486.0	8.60E-22	1.000	488.0	9.10E-22	1.000	490.0	9.70E-22	1.000	492.0	1.02E-21	1.000
494.0	1.07E-21	1.000	496.0	1.12E-21	1.000	498.0	1.17E-21	1.000	500.0	1.22E-21	1.000	502.0	1.28E-21	1.000
504.0	1.33E-21	1.000	506.0	1.39E-21	1.000	508.0	1.44E-21	1.000	510.0	1.50E-21	1.000	512.0	1.56E-21	1.000
514.0	1.61E-21	1.000	516.0	1.67E-21	1.000	518.0	1.72E-21	1.000	520.0	1.78E-21	1.000	522.0	1.89E-21	1.000
524.0	2.00E-21	1.000	526.0	2.11E-21	1.000	528.0	2.22E-21	1.000	530.0	2.33E-21	1.000	532.0	2.44E-21	1.000
534.0	2.55E-21	1.000	536.0	2.66E-21	1.000	538.0	2.77E-21	1.000	540.0	2.88E-21	1.000	542.0	2.98E-21	1.000
544.0	3.08E-21	1.000	546.0	3.18E-21	1.000	548.0	3.28E-21	1.000	550.0	3.38E-21	1.000	552.0	3.48E-21	1.000
554.0	3.58E-21	1.000	556.0	3.68E-21	1.000	558.0	3.78E-21	1.000	560.0	3.88E-21	1.000	562.0	3.95E-21	1.000
564.0	4.01E-21	1.000	566.0	4.08E-21	1.000	568.0	4.15E-21	1.000	570.0	4.22E-21	1.000	572.0	4.28E-21	1.000
574.0	4.35E-21	1.000	576.0	4.42E-21	1.000	578.0	4.48E-21	1.000	580.0	4.55E-21	1.000	582.0	4.58E-21	1.000
584.0	4.62E-21	1.000	586.0	4.65E-21	1.000	588.0	4.69E-21	1.000	590.0	4.72E-21	1.000	592.0	4.75E-21	1.000
594.0	4.79E-21	1.000	596.0	4.82E-21	1.000	598.0	4.86E-21	1.000	600.0	4.89E-21	1.000	602.0	4.79E-21	1.000
604.0	4.69E-21	1.000	606.0	4.59E-21	1.000	608.0	4.49E-21	1.000	610.0	4.40E-21	1.000	612.0	4.30E-21	1.000
614.0	4.20E-21	1.000	616.0	4.10E-21	1.000	618.0	4.00E-21	1.000	620.0	3.90E-21	1.000	622.0	3.78E-21	1.000
624.0	3.67E-21	1.000	626.0	3.55E-21	1.000	628.0	3.44E-21	1.000	630.0	3.32E-21	1.000	632.0	3.20E-21	1.000
634.0	3.09E-21	1.000	636.0	2.97E-21	1.000	638.0	2.86E-21	1.000	640.0	2.74E-21	1.000	642.0	2.67E-21	1.000
644.0	2.61E-21	1.000	646.0	2.54E-21	1.000	648.0	2.47E-21	1.000	650.0	2.41E-21	1.000	652.0	2.34E-21	1.000
654.0	2.27E-21	1.000	656.0	2.20E-21	1.000	658.0	2.14E-21	1.000	660.0	2.07E-21	1.000	662.0	2.00E-21	1.000
664.0	1.93E-21	1.000	666.0	1.86E-21	1.000	668.0	1.79E-21	1.000	670.0	1.72E-21	1.000	672.0	1.65E-21	1.000
674.0	1.58E-21	1.000	676.0	1.51E-21	1.000	678.0	1.44E-21	1.000	680.0	1.37E-21	1.000	682.0	1.32E-21	1.000
684.0	1.28E-21	1.000	686.0	1.23E-21	1.000	688.0	1.19E-21	1.000	690.0	1.14E-21	1.000	692.0	1.10E-21	1.000
694.0	1.05E-21	1.000	696.0	1.00E-21	1.000	698.0	9.60E-22	1.000	700.0	9.10E-22	1.000	702.0	8.90E-22	1.000
704.0	8.60E-22	1.000	706.0	8.30E-22	1.000	708.0	8.00E-22	1.000	710.0	7.80E-22	1.000	712.0	7.50E-22	1.000
714.0	7.20E-22	1.000	716.0	6.90E-22	1.000	718.0	6.70E-22	1.000	720.0	6.40E-22	1.000	722.0	6.10E-22	1.000
724.0	5.90E-22	1.000	726.0	5.70E-22	1.000	728.0	5.50E-22	1.000	730.0	5.10E-22	1.000	732.0	0.00E+00	1.000

Photolysis File = HONOCB

WL (nm)	Abs (cm^2)	QY	WL (nm)	Abs (cm^2)	QY	WL (nm)	Abs (cm^2)	QY	WL (nm)	Abs (cm^2)	QY	WL (nm)	Abs (cm^2)	QY
311.0	0.00E+00	1.000	312.0	2.00E-21	1.000	313.0	4.20E-21	1.000	314.0	4.60E-21	1.000	315.0	4.20E-21	1.000
316.0	3.00E-21	1.000	317.0	4.60E-21	1.000	318.0	3.60E-20	1.000	319.0	6.10E-20	1.000	320.0	2.10E-20	1.000
321.0	4.27E-20	1.000	322.0	4.01E-20	1.000	323.0	3.93E-20	1.000	324.0	4.01E-20	1.000	325.0	4.04E-20	1.000
326.0	3.13E-20	1.000	327.0	4.12E-20	1.000	328.0	7.55E-20	1.000	329.0	6.64E-20	1.000	330.0	7.29E-20	1.000
331.0	8.70E-20	1.000	332.0	1.38E-19	1.000	333.0	5.91E-20	1.000	334.0	5.91E-20	1.000	335.0	6.45E-20	1.000
336.0	5.91E-20	1.000	337.0	4.58E-20	1.000	338.0	1.91E-19	1.000	339.0	1.63E-19	1.000	340.0	1.05E-19	1.000
341.0	8.70E-20	1.000	342.0	3.35E-19	1.000	343.0	2.01E-19	1.000	344.0	1.02E-19	1.000	345.0	8.54E-20	1.000
346.0	8.32E-20	1.000	347.0	8.20E-20	1.000	348.0	7.49E-20	1.000	349.0	7.13E-20	1.000	350.0	6.83E-20	1.000
351.0	1.74E-19	1.000	352.0	1.14E-19	1.000	353.0	3.71E-19	1.000	354.0	4.96E-19	1.000	355.0	2.46E-19	1.000
356.0	1.19E-19	1.000	357.0	9.35E-20	1.000	358.0	7.78E-20	1.000	359.0	7.29E-20	1.000	360.0	6.83E-20	1.000
361.0	6.90E-20	1.000	362.0	7.32E-20	1.000	363.0	9.00E-20	1.000	364.0	1.21E-19	1.000	365.0	1.33E-19	1.000
366.0	2.13E-19	1.000	367.0	3.52E-19	1.000	368.0	4.50E-19	1.000	369.0	2.93E-19	1.000	370.0	1.19E-19	1.000
371.0	9.46E-20	1.000	372.0	8.85E-20	1.000	373.0	7.44E-20	1.000	374.0	4.77E-20	1.000	375.0	2.70E-20	1.000
376.0	1.90E-20	1.000	377.0	1.50E-20	1.000	378.0	1.90E-20	1.000	379.0	5.80E-20	1.000	380.0	7.78E-20	1.000
381.0	1.14E-19	1.000	382.0	1.40E-19	1.000	383.0	1.72E-19	1.000	384.0	1.99E-19	1.000	385.0	1.90E-19	1.000
386.0	1.19E-19	1.000	387.0	5.65E-20	1.000	388.0	3.20E-20	1.000	389.0	1.90E-20	1.000	390.0	1.20E-20	1.000
391.0	5.00E-21	1.000	392.0	0.00E+00	1.000									

Table 7 (continued)

Photolysis File = H2O2CB

WL (nm)	Abs (cm^2)	QY	WL (nm)	Abs (cm^2)	QY	WL (nm)	Abs (cm^2)	QY	WL (nm)	Abs (cm^2)	QY	WL (nm)	Abs (cm^2)	QY
280.0	2.09E-20	1.000	281.0	2.00E-20	1.000	282.0	1.90E-20	1.000	283.0	1.81E-20	1.000	284.0	1.71E-20	1.000
285.0	1.62E-20	1.000	286.0	1.54E-20	1.000	287.0	1.46E-20	1.000	288.0	1.39E-20	1.000	289.0	1.31E-20	1.000
290.0	1.23E-20	1.000	291.0	1.17E-20	1.000	292.0	1.11E-20	1.000	293.0	1.05E-20	1.000	294.0	9.92E-21	1.000
295.0	9.33E-21	1.000	296.0	8.88E-21	1.000	297.0	8.43E-21	1.000	298.0	7.98E-21	1.000	299.0	7.53E-21	1.000
300.0	7.08E-21	1.000	301.0	6.74E-21	1.000	302.0	6.40E-21	1.000	303.0	6.06E-21	1.000	304.0	5.72E-21	1.000
305.0	5.38E-21	1.000	306.0	5.14E-21	1.000	307.0	4.90E-21	1.000	308.0	4.65E-21	1.000	309.0	4.41E-21	1.000
310.0	4.17E-21	1.000	311.0	3.97E-21	1.000	312.0	3.77E-21	1.000	313.0	3.56E-21	1.000	314.0	3.36E-21	1.000
315.0	3.16E-21	1.000	316.0	3.02E-21	1.000	317.0	2.88E-21	1.000	318.0	2.73E-21	1.000	319.0	2.59E-21	1.000
320.0	2.45E-21	1.000	321.0	2.33E-21	1.000	322.0	2.21E-21	1.000	323.0	2.10E-21	1.000	324.0	1.98E-21	1.000
325.0	1.86E-21	1.000	326.0	1.77E-21	1.000	327.0	1.68E-21	1.000	328.0	1.59E-21	1.000	329.0	1.50E-21	1.000
330.0	1.41E-21	1.000	331.0	1.35E-21	1.000	332.0	1.29E-21	1.000	333.0	1.22E-21	1.000	334.0	1.16E-21	1.000
335.0	1.10E-21	1.000	336.0	1.05E-21	1.000	337.0	9.90E-22	1.000	338.0	9.40E-22	1.000	339.0	8.90E-22	1.000
340.0	8.30E-22	1.000	341.0	7.90E-22	1.000	342.0	7.50E-22	1.000	343.0	7.10E-22	1.000	344.0	6.70E-22	1.000
345.0	6.30E-22	1.000	346.0	6.00E-22	1.000	347.0	5.70E-22	1.000	348.0	5.40E-22	1.000	349.0	5.10E-22	1.000
350.0	4.80E-22	1.000	351.0	0.00E+00	1.000									

Photolysis File = NO3CBEST

400.0	0.00E+00	1.000	405.0	3.00E-20	1.000	410.0	4.00E-20	1.000	415.0	5.00E-20	1.000	420.0	8.00E-20	1.000
425.0	1.00E-19	1.000	430.0	1.30E-19	1.000	435.0	1.80E-19	1.000	440.0	1.90E-19	1.000	445.0	2.20E-19	1.000
450.0	2.80E-19	1.000	455.0	3.30E-19	1.000	460.0	3.70E-19	1.000	465.0	4.30E-19	1.000	470.0	5.10E-19	1.000
475.0	6.00E-19	1.000	480.0	6.40E-19	1.000	485.0	6.90E-19	1.000	490.0	8.80E-19	1.000	495.0	9.50E-19	1.000
500.0	1.01E-18	1.000	505.0	1.10E-18	1.000	510.0	1.32E-18	1.000	515.0	1.40E-18	1.000	520.0	1.45E-18	1.000
525.0	1.48E-18	1.000	530.0	1.94E-18	1.000	535.0	2.04E-18	1.000	540.0	1.81E-18	1.000	545.0	1.81E-18	1.000
550.0	2.36E-18	1.000	555.0	2.68E-18	1.000	560.0	3.07E-18	1.000	565.0	2.53E-18	1.000	570.0	2.54E-18	1.000
575.0	2.74E-18	1.000	580.0	3.05E-18	1.000	585.0	2.77E-18	1.000	590.0	5.14E-18	1.000	595.0	4.08E-18	1.000
600.0	2.83E-18	1.000	605.0	3.45E-18	1.000	610.0	1.45E-18	1.000	615.0	1.96E-18	1.000	620.0	3.58E-18	1.000
625.0	9.25E-18	1.000	630.0	5.66E-18	1.000	635.0	1.45E-18	1.000	640.0	1.11E-18	1.000	645.0	0.00E+00	1.000

Photolysis File = HCHORBCB

280.0	2.34E-20	0.560	281.0	1.65E-20	0.580	282.0	7.60E-21	0.600	283.0	4.60E-21	0.620	284.0	3.93E-20	0.630
285.0	3.46E-20	0.650	286.0	2.32E-20	0.670	287.0	9.50E-21	0.680	288.0	2.32E-20	0.700	289.0	2.50E-20	0.710
290.0	1.43E-20	0.720	291.0	1.32E-20	0.730	292.0	6.60E-21	0.750	293.0	5.22E-20	0.760	294.0	4.30E-20	0.760
295.0	3.21E-20	0.770	296.0	1.59E-20	0.780	297.0	1.96E-20	0.790	298.0	3.66E-20	0.790	299.0	1.55E-20	0.790
300.0	7.20E-21	0.800	301.0	1.51E-20	0.800	302.0	7.40E-21	0.800	303.0	4.35E-20	0.800	304.0	4.79E-20	0.800
305.0	4.94E-20	0.790	306.0	3.02E-20	0.790	307.0	1.16E-20	0.790	308.0	2.18E-20	0.780	309.0	2.25E-20	0.770
310.0	1.03E-20	0.760	311.0	8.10E-21	0.750	312.0	1.49E-20	0.740	313.0	1.55E-20	0.730	314.0	3.99E-20	0.720
315.0	2.88E-20	0.700	316.0	2.79E-20	0.690	317.0	3.59E-20	0.670	318.0	1.65E-20	0.650	319.0	7.30E-21	0.630
320.0	1.71E-20	0.610	321.0	1.32E-20	0.590	322.0	4.30E-21	0.570	323.0	6.00E-21	0.540	324.0	7.50E-21	0.510
325.0	2.19E-20	0.490	326.0	3.44E-20	0.460	327.0	1.75E-20	0.430	328.0	1.01E-20	0.390	329.0	3.03E-20	0.360
330.0	1.96E-20	0.330	331.0	7.90E-21	0.290	332.0	3.20E-21	0.250	333.0	1.50E-21	0.210	334.0	1.70E-21	0.170
335.0	2.00E-22	0.130	336.0	1.70E-21	0.083	337.0	3.20E-21	0.038	338.0	1.93E-20	0.000	339.0	2.15E-20	0.000
340.0	1.07E-20	0.000												

Photolysis File = HCHORMCB

280.0	2.69E-20	0.560	281.0	1.34E-20	0.580	282.0	9.80E-21	0.600	283.0	5.80E-21	0.620	284.0	2.78E-20	0.630
285.0	4.10E-20	0.650	286.0	1.95E-20	0.670	287.0	1.01E-20	0.680	288.0	2.23E-20	0.700	289.0	3.20E-20	0.710
290.0	1.09E-20	0.720	291.0	1.88E-20	0.730	292.0	5.80E-21	0.750	293.0	1.81E-20	0.760	294.0	5.45E-20	0.760
295.0	3.98E-20	0.770	296.0	2.15E-20	0.780	297.0	1.12E-20	0.790	298.0	4.46E-20	0.790	299.0	2.53E-20	0.790
300.0	5.30E-21	0.800	301.0	1.15E-20	0.800	302.0	1.24E-20	0.800	303.0	2.41E-20	0.800	304.0	7.36E-20	0.800
305.0	4.40E-20	0.790	306.0	5.01E-20	0.790	307.0	2.90E-20	0.790	308.0	1.33E-20	0.780	309.0	2.78E-20	0.770
310.0	2.65E-20	0.760	311.0	8.40E-21	0.750	312.0	8.70E-21	0.740	313.0	1.15E-20	0.730	314.0	5.07E-20	0.720
315.0	4.83E-20	0.700	316.0	2.65E-20	0.690	317.0	6.15E-20	0.670	318.0	3.62E-20	0.650	319.0	1.18E-20	0.630
320.0	9.90E-21	0.610	321.0	1.59E-20	0.590	322.0	9.00E-21	0.570	323.0	2.10E-21	0.540	324.0	6.00E-21	0.510
325.0	6.40E-21	0.490	326.0	3.74E-20	0.460	327.0	5.67E-20	0.430	328.0	3.14E-20	0.390	329.0	1.06E-20	0.360
330.0	4.46E-20	0.330	331.0	2.53E-20	0.290	332.0	6.60E-21	0.250	333.0	2.20E-21	0.210	334.0	1.00E-21	0.170
335.0	8.00E-22	0.130	336.0	1.00E-21	0.083	337.0	3.10E-21	0.038	338.0	1.09E-20	0.000	339.0	4.71E-20	0.000
340.0	2.78E-20	0.000												

Photolysis File = HCHOSBCB

280.0	2.34E-20	0.440	281.0	1.65E-20	0.420	282.0	7.60E-21	0.400	283.0	4.60E-21	0.380	284.0	3.93E-20	0.370
285.0	3.46E-20	0.350	286.0	2.32E-20	0.330	287.0	9.50E-21	0.320	288.0	2.32E-20	0.300	289.0	2.50E-20	0.290
290.0	1.43E-20	0.280	291.0	1.32E-20	0.270	292.0	6.60E-21	0.250	293.0	5.22E-20	0.240	294.0	4.30E-20	0.240
295.0	3.21E-20	0.230	296.0	1.59E-20	0.220	297.0	1.96E-20	0.210	298.0	3.66E-20	0.210	299.0	1.55E-20	0.210
300.0	7.20E-21	0.200	301.0	1.51E-20	0.200	302.0	7.40E-21	0.200	303.0	4.35E-20	0.200	304.0	4.79E-20	0.200
305.0	4.94E-20	0.210	306.0	3.02E-20	0.210	307.0	1.16E-20	0.210	308.0	2.18E-20	0.220	309.0	2.25E-20	0.230
310.0	1.03E-20	0.240	311.0	8.10E-21	0.250	312.0	1.49E-20	0.260	313.0	1.55E-20	0.270	314.0	3.99E-20	0.280
315.0	2.88E-20	0.300	316.0	2.79E-20	0.310	317.0	3.59E-20	0.330	318.0	1.65E-20	0.350	319.0	7.30E-21	0.370
320.0	1.71E-20	0.390	321.0	1.32E-20	0.410	322.0	4.30E-21	0.430	323.0	6.00E-21	0.460	324.0	7.50E-21	0.490
325.0	2.19E-20	0.510	326.0	3.44E-20	0.540	327.0	1.75E-20	0.550	328.0	1.01E-20	0.570	329.0	3.03E-20	0.580
330.0	1.96E-20	0.590	331.0	7.90E-21	0.600	332.0	3.20E-21	0.610	333.0	1.50E-21	0.620	334.0	1.70E-21	0.620
335.0	2.00E-22	0.620	336.0	1.70E-21	0.620	337.0	3.20E-21	0.620	338.0	1.93E-20	0.610	339.0	2.15E-20	0.610
340.0	1.07E-20	0.600	341.0	3.10E-21	0.590	342.0	9.40E-21	0.570	343.0	1.37E-20	0.560	344.0	5.70E-21	0.540
345.0	1.20E-21	0.520	346.0	4.00E-22	0.500	347.0	4.00E-22	0.470	348.0	7.00E-22	0.450	349.0	3.00E-22	0.420
350.0	3.00E-22	0.390	351.0	9.00E-22	0.360	352.0	9.00E-21	0.330	353.0	1.17E-20	0.300	354.0	7.20E-21	0.260
355.0	2.60E-21	0.230	356.0	5.00E-22	0.200	357.0	3.00E-22	0.160	358.0	4.00E-22	0.130	359.0	3.00E-22	0.100
360.0	0.00E+00	0.063												

Table 7 (continued)

WL (nm)	Abs (cm^2)	QY	WL (nm)	Abs (cm^2)	QY	WL (nm)	Abs (cm^2)	QY	WL (nm)	Abs (cm^2)	QY	WL (nm)	Abs (cm^2)	QY
Photolysis File = HCHOSMCB														
280.0	2.69E-20	0.440	281.0	1.34E-20	0.420	282.0	9.80E-21	0.400	283.0	5.80E-21	0.380	284.0	2.78E-20	0.370
285.0	4.10E-20	0.350	286.0	1.95E-20	0.330	287.0	1.01E-20	0.320	288.0	2.23E-20	0.300	289.0	3.20E-20	0.290
290.0	1.09E-20	0.280	291.0	1.88E-20	0.270	292.0	5.80E-21	0.250	293.0	1.81E-20	0.240	294.0	5.45E-20	0.240
295.0	3.98E-20	0.230	296.0	2.15E-20	0.220	297.0	1.12E-20	0.210	298.0	4.46E-20	0.210	299.0	2.53E-20	0.210
300.0	5.30E-21	0.200	301.0	1.15E-20	0.200	302.0	1.24E-20	0.200	303.0	2.41E-20	0.200	304.0	7.36E-20	0.200
305.0	4.40E-20	0.210	306.0	5.01E-20	0.210	307.0	2.90E-20	0.210	308.0	1.33E-20	0.220	309.0	2.78E-20	0.230
310.0	2.65E-20	0.240	311.0	8.40E-21	0.250	312.0	8.70E-21	0.260	313.0	1.15E-20	0.270	314.0	5.07E-20	0.280
315.0	4.83E-20	0.300	316.0	2.65E-20	0.310	317.0	6.15E-20	0.330	318.0	3.62E-20	0.350	319.0	1.18E-20	0.370
320.0	9.90E-21	0.390	321.0	1.59E-20	0.410	322.0	9.00E-21	0.430	323.0	2.10E-21	0.460	324.0	6.00E-21	0.490
325.0	6.40E-21	0.510	326.0	3.74E-20	0.540	327.0	5.67E-20	0.550	328.0	3.14E-20	0.570	329.0	1.06E-20	0.580
330.0	4.46E-20	0.590	331.0	2.53E-20	0.600	332.0	6.60E-21	0.610	333.0	2.20E-21	0.620	334.0	1.00E-21	0.620
335.0	8.00E-22	0.620	336.0	1.00E-21	0.620	337.0	3.10E-21	0.620	338.0	1.09E-20	0.610	339.0	4.71E-20	0.610
340.0	2.78E-20	0.600	341.0	9.00E-21	0.590	342.0	3.30E-21	0.570	343.0	2.09E-20	0.560	344.0	1.45E-20	0.540
345.0	3.70E-21	0.520	346.0	6.00E-22	0.500	347.0	0.00E+00	0.470	348.0	5.00E-22	0.450	349.0	2.00E-22	0.420
350.0	0.00E+00	0.390	351.0	0.00E+00	0.360	352.0	6.00E-22	0.330	353.0	1.57E-20	0.300	354.0	2.35E-20	0.260
355.0	1.33E-20	0.230	356.0	3.40E-21	0.200	357.0	8.00E-22	0.160	358.0	2.00E-22	0.130	359.0	0.00E+00	0.100
360.0	0.00E+00	0.063												
Photolysis File = ALD2RCB														
280.0	4.50E-20	0.580	281.0	4.54E-20	0.575	282.0	4.58E-20	0.570	283.0	4.62E-20	0.565	284.0	4.66E-20	0.560
285.0	4.70E-20	0.555	286.0	4.74E-20	0.550	287.0	4.78E-20	0.545	288.0	4.82E-20	0.540	289.0	4.86E-20	0.535
290.0	4.90E-20	0.530	291.0	4.82E-20	0.520	292.0	4.74E-20	0.510	293.0	4.66E-20	0.500	294.0	4.58E-20	0.490
295.0	4.50E-20	0.480	296.0	4.46E-20	0.470	297.0	4.42E-20	0.460	298.0	4.38E-20	0.450	299.0	4.34E-20	0.440
300.0	4.30E-20	0.430	301.0	4.12E-20	0.418	302.0	3.94E-20	0.406	303.0	3.76E-20	0.394	304.0	3.58E-20	0.382
305.0	3.40E-20	0.370	306.0	3.27E-20	0.350	307.0	3.14E-20	0.330	308.0	3.01E-20	0.310	309.0	2.88E-20	0.290
310.0	2.75E-20	0.270	311.0	2.62E-20	0.250	312.0	2.49E-20	0.230	313.0	2.36E-20	0.210	314.0	2.23E-20	0.190
315.0	2.10E-20	0.170	316.0	2.04E-20	0.156	317.0	1.98E-20	0.142	318.0	1.92E-20	0.128	319.0	1.86E-20	0.114
320.0	1.80E-20	0.100	321.0	1.66E-20	0.088	322.0	1.52E-20	0.076	323.0	1.38E-20	0.064	324.0	1.24E-20	0.052
325.0	1.10E-20	0.040	326.0	1.18E-20	0.032	327.0	9.36E-21	0.024	328.0	8.54E-21	0.016	329.0	7.72E-21	0.008
330.0	6.90E-21	0.000												

for this specific set of experiments as indicated in Appendix A. Where possible, the parameters were derived based on analysis of results of characterization experiments carried out in conjunction with these runs. In cases where no data are available for this specific chamber, the parameters used by Carter and Lurmann (1991) for model simulations of runs carried out in the SAPRC ITC chamber were used. The SAPRC ITC is similar in construction to the SAPRC ETC used for this study; both are indoor chambers consisting of 2-mil thick FEP Teflon reaction bags with blacklight light source. The specific chamber-dependent parameters used in chamber model simulations for this study, and their derivations are discussed in Appendix A, and included in the reaction listings for the base case mechanisms in Table 2 and 6. The same chamber model was used for both base case mechanisms.

RESULTS AND DISCUSSION

Experimental Results

A total of 4 mini-surrogate-NO_x experiments with added isoprene were carried out, each alternating with a standard (or "base case") mini-surrogate-NO_x experiment which did not have the added isoprene. In addition, since the experiments were carried out in conjunction with similar runs with other VOCs, the relevant base case runs conducted before and after those carried out for this program are also included in the data analysis. This provides the most comprehensive available baseline against which to compare the effects of the added isoprene.

Typical results are shown in Figures 1 and 2. Figure 1 gives concentration-time profiles of species measured during a representative standard run, along with results of model simulations using the adjusted SAPRC-91 discussed in the previous section. Note that the standard run does not form an ozone maximum, since ozone is continuing to form at the end of the experiments. This is characteristic of "maximum reactivity" conditions, where the addition of VOCs has the greatest effect on ozone formation (Carter, 1991). The results of the other standard runs are similar, though there is some variation from run to run because of run to run variations of temperature and (to a lesser extent) other reaction conditions. These variations, and the methods used to take them into account when deriving the measured incremental reactivities, are discussed in Appendix A.

Figure 2 shows concentration-time profiles for selected species measured during a selected added isoprene run, along with profiles for the same species (except for isoprene) measured during the standard run immediately preceding it. The added isoprene can be seen to cause an increase in the rate of NO consumption and the amount of ozone formed during the experiment, and also causes a slight but measurable increase in the rate of m-xylene consumption, relative to the standard run. The results of the other added isoprene experiments are similar.

Table 8 gives a summary of the results of all the added isoprene runs and of the standard runs conducted during the same period, with the runs listed in chronological order. The table gives the average temperatures, the initial reactant concentrations, the d(O_3-NO) (i.e., ozone formed + NO oxidized) results at 2, 4, and 6 hours, the final IntOH results derived as discussed in the previous sections, and the ratio of the final d(O_3-NO) to the final IntOH (designated ConvR on the table, following the terminology in Appendix A).

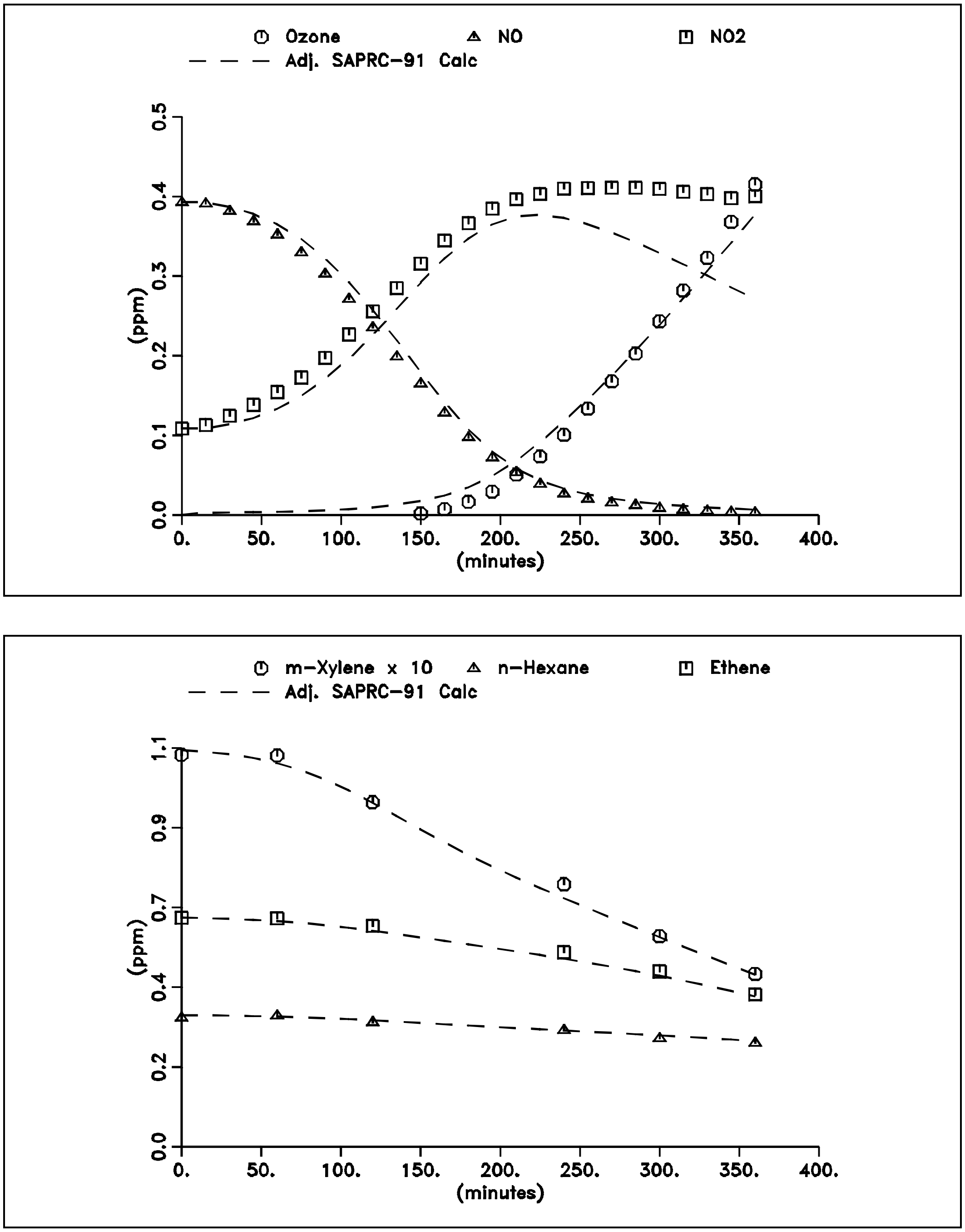

Figure 1. Concentration-time profiles of species measured during the representative Set 3 standard run ETC-292. Results of model calculations using the adjusted SAPRC-91 mechanism are also shown.

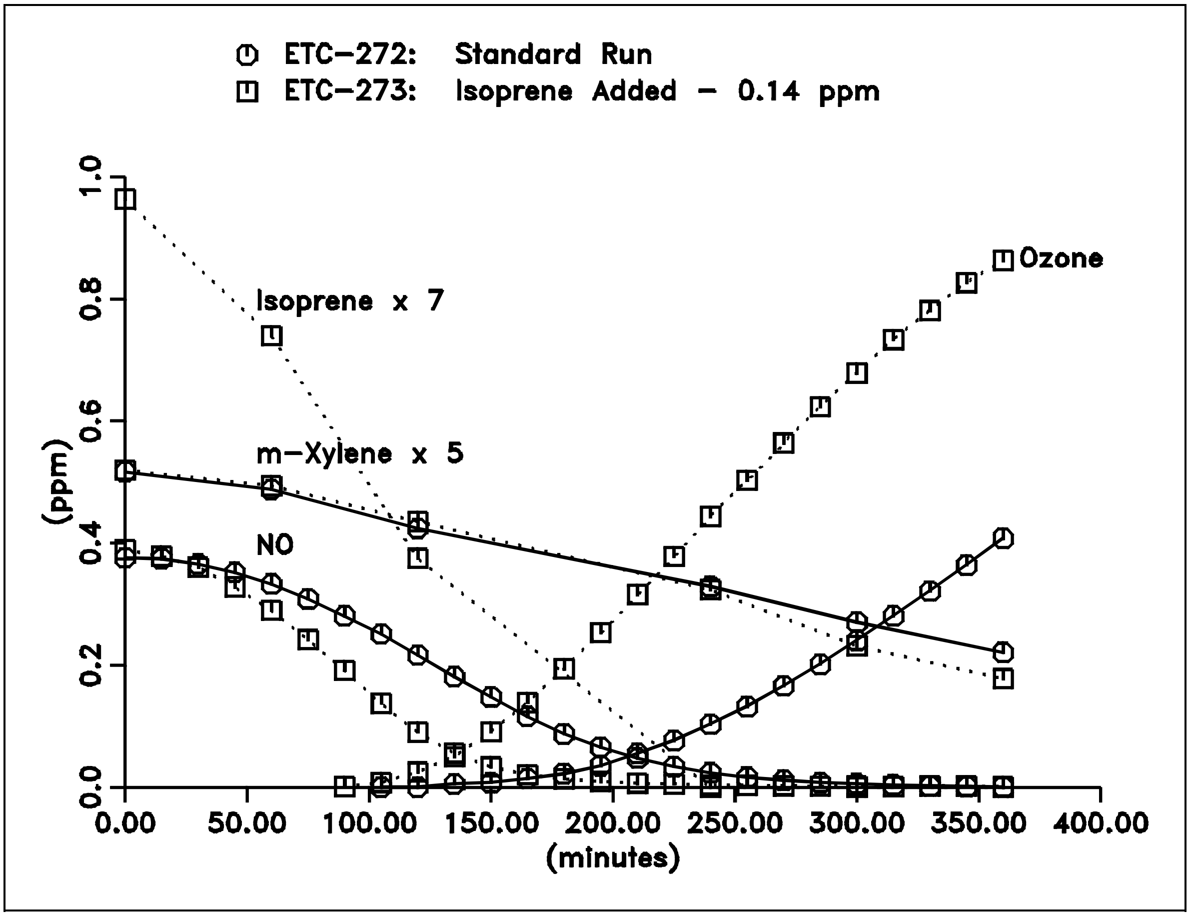

Figure 2. Concentration-time profiles of selected species measured during a selected added isoprene run and during the standard run immediately preceding it.

Table 8. Conditions and Selected Results of the Mini-Surrogate Runs used for Isoprene Reactivity Assessment

Run	Added (ppm)	Avg.T (K)	Initial Conc (ppb) NO	NO2	n-C_6	Ethe.	m-Xyl	d(O_3-NO) (ppb) t=2	t=4	t=6	IntOH (ppt-min)	ConvR [a] (10^3 min^{-1})
270	----	301.2	382	105	384	681	96.1	163	442	762	22.8 ± 8%	33.5
271	**0.157**	**300.1**	**377**	**115**	**387**	**674**	**99.4**	**303**	**788**	**1207**	**28.6 ± 7%**	**42.3**
272	----	301.2	376	119	394	665	103.4	163	458	787	23.8 ± 8%	33.0
273	**0.139**	**301.7**	**389**	**108**	**376**	**653**	**103.9**	**334**	**840**	**1262**	**30.3 ± 8%**	**41.7**
274	----	302.3	397	112	381	659	103.3	159	479	839	23.2 ± 8%	36.2
275	**0.109**	**302.2**	**392**	**114**	**363**	**647**	**98.0**	**297**	**765**	**1217**	**30.8 ± 8%**	**39.6**
276	----	302.3	382	113	365	648	98.9	163	468	819	25.6 ± 7%	32.0
277	**0.076**	**303.1**	**390**	**113**	**364**	**645**	**98.8**	**268**	**701**	**1167**	**29.9 ± 6%**	**39.0**
278	----	302.8	394	119	364	635	98.9	153	456	826	23.3 ± 8%	35.4

[a] ConvR is the ratio of the 6-hour d(O_3-NO) to the 6-hour IntOH. It is assumed to have the same relative uncertainty as the IntOH.

The details of the reactivity analyses of each of the added isoprene runs are given on Tables 9-11. Tables 9 and 10 give the results for $d(O_3\text{-}NO)$ and IntOH reactivities, respectively, and the data used to derive them. Specifically, for each added isoprene run, these tables give:

- the amount of isoprene added and (for Table 9) its estimated uncertainty;
- the amount of isoprene reacted at each hour of the run and its estimated uncertainty;
- the hourly $d(O_3\text{-}NO)$ or IntOH results from the added isoprene run, and (for IntOH) the measurement uncertainties;
- the hourly $d(O_3\text{-}NO)$ or IntOH predicted, using a linear least squares regression analysis of the base case results against temperature, etc., to occur in a base case run carried out under the conditions of the added isoprene run, and the uncertainty of the prediction of the regression;
- the change in hourly $d(O_3\text{-}NO)$ or IntOH attributed to the addition of the isoprene, i.e., the difference between the hourly $d(O_3\text{-}NO)$ or IntOH for the added isoprene run and the corresponding predicted for the base case run, and the estimated uncertainty;
- the hourly $d(O_3\text{-}NO)$ or IntOH incremental reactivities, calculated by dividing the change in hourly $d(O_3\text{-}NO)$ or IntOH attributed to the added isoprene by the amount of isoprene added, and their uncertainties; and
- the hourly $d(O_3\text{-}NO)$ or IntOH mechanistic reactivities, calculated by dividing the change in hourly $d(O_3\text{-}NO)$ or IntOH attributed to the addition of the isoprene by the amount of isoprene reacted, and their uncertainties.

Table 11 gives the results for the direct incremental and direct mechanistic (ConvF) reactivities and the data used to derive them. In addition to the amounts of isoprene added and reacted, it gives:

- the final IntOH for the added isoprene run, which is used in Equation (V) to calculate, $d(O_3\text{-}NO)^{\text{base ROG (test)}}$, and its measurement uncertainty;
- the $d(O_3\text{-}NO)^{\text{base}}/\text{IntOH}^{\text{base}}$ ratio estimated, using a linear least squares regression analysis of this ratio for the base case runs, to correspond to the conditions of the added isoprene experiment, and its estimated uncertainty from the regression;
- the $d(O_3\text{-}NO)^{\text{base ROG (test)}}$ value estimated using the above two quantities and Equation (V), and its uncertainty;
- the final $d(O_3\text{-}NO)^{\text{test}}$ of the added isoprene run;
- the direct incremental reactivity, calculated as indicated on footnote [c] to the table; and
- the ConvF reactivity, calculated from the quantities on the table using Equation (VIII), and its estimated uncertainty.

Table 9. Derivation of Isoprene Reactivities with Respect to Hourly Ozone Formation and NO Oxidation.

Run	Added (ppm)	Time (hr)	Reacted [a] (ppm)	Reacted [a] Deriv.	$d(O_3\text{-}NO)$ (ppm) Test	$d(O_3\text{-}NO)$ (ppm) Base Fit	$d(O_3\text{-}NO)$ (ppm) Change	Reactivity (mol/mol) Incremental	Reactivity (mol/mol) Mechanistic
277	0.076 ±0.002	1	0.016 ±0.002	D(d2)	0.079	0.043 ±0.008	0.036 ±0.012	0.48 ± 32%	2.23 ± 34%
		2	0.043 ±0.002	D(d2)	0.268	0.163 ±0.016	0.105 ±0.023	1.38 ± 22%	2.46 ± 22%
		3	0.058 ±0.002	D(d2)	0.476	0.320 ±0.023	0.156 ±0.033	2.1 ± 21%	2.68 ± 21%
		4	0.075 ±0.002	D(d2)	0.701	0.471 ±0.034	0.230 ±0.048	3.0 ± 21%	3.06 ± 21%
		5	0.075 ±0.002	D(d2)	0.944	0.639 ±0.039	0.305 ±0.055	4.0 ± 18%	4.05 ± 18%
		6	0.075 ±0.002	D(d2)	1.167	0.829 ±0.047	0.338 ±0.067	4.4 ± 20%	4.48 ± 20%
275	0.108 ±0.002	1	0.028 ±0.003	D(d2)	0.097	0.041 ±0.008	0.056 ±0.012	0.52 ± 21%	2.02 ± 23%
		2	0.064 ±0.002	D(d2)	0.297	0.153 ±0.016	0.144 ±0.023	1.33 ± 16%	2.24 ± 16%
		3	0.086 ±0.002	D(d2)	0.523	0.301 ±0.023	0.222 ±0.033	2.0 ± 15%	2.58 ± 15%
		4	0.108 ±0.002	D(d2)	0.765	0.446 ±0.034	0.319 ±0.048	2.9 ± 15%	2.97 ± 15%
		5	0.108 ±0.002	D(d2)	1.010	0.601 ±0.038	0.409 ±0.054	3.8 ± 13%	3.80 ± 13%
		6	0.108 ±0.002	D(d2)	1.217	0.776 ±0.047	0.441 ±0.066	4.1 ± 15%	4.10 ± 15%
273	0.139 ±0.004	1	0.035 ±0.006	D(d2)	0.103	0.039 ±0.008	0.064 ±0.012	0.46 ± 18%	1.83 ± 24%
		2	0.084 ±0.005	D(d2)	0.334	0.151 ±0.016	0.183 ±0.022	1.31 ± 13%	2.16 ± 14%
		3	0.111 ±0.005	D(d2)	0.580	0.297 ±0.023	0.283 ±0.032	2.0 ± 12%	2.54 ± 12%
		4	0.138 ±0.004	D(d2)	0.840	0.441 ±0.033	0.399 ±0.047	2.9 ± 12%	2.89 ± 12%
		5	0.138 ±0.004	D(d2)	1.076	0.592 ±0.038	0.484 ±0.054	3.5 ± 12%	3.50 ± 12%
		6	0.138 ±0.004	D(d2)	1.262	0.762 ±0.047	0.500 ±0.066	3.6 ± 14%	3.62 ± 14%
271	0.157 ±0.007	1	0.039 ±0.009	D(d2)	0.101	0.036 ±0.008	0.065 ±0.012	0.42 ± 18%	1.66 ± 29%
		2	0.091 ±0.008	D(d2)	0.303	0.133 ±0.016	0.170 ±0.022	1.09 ± 14%	1.87 ± 16%
		3	0.123 ±0.007	D(d2)	0.540	0.261 ±0.023	0.279 ±0.032	1.78 ± 12%	2.27 ± 13%
		4	0.139 ±0.007	D(d2)	0.788	0.391 ±0.033	0.397 ±0.047	2.5 ± 13%	2.85 ± 13%
		5	0.147 ±0.007	D(d2)	1.021	0.519 ±0.038	0.502 ±0.054	3.2 ± 12%	3.41 ± 12%
		6	0.150 ±0.007	D(d2)	1.207	0.661 ±0.047	0.546 ±0.066	3.5 ± 13%	3.63 ± 13%

[a] Codes for methods for deriving amounts reacted are as follows: "IntOH" = derived using IntOH and the OH radical rate constant for the VOC; "D(tn)" or "D(dn)" = amounts reacted determined directly from the measured data for the VOC, where the data was smoothed by fitting to linear (n=2) or quadratic (n=3) functions of time "(tn)" or d(O3-NO) "(dn)".

Table 10. Derivation of Reactivities with Respect to Hourly Integrated OH Radical Levels for All Test VOC Experiments.

Run	Added (ppm)	Time (hr)	Reacted (ppm)	IntOH (ppt-min) Test Run	IntOH (ppt-min) Base Fit	IntOH (ppt-min) Change	Reactivity (ppt-min/ppm) Incremental	Reactivity (ppt-min/ppm) Mechanistic
277	0.076	1	0.016 ±0.002	1.0 ±0.8	1.3 ±0.6	-0.2 ±1.0	(-3. ± 13.)	(-14. ± 63.)
		2	0.043 ±0.002	3.7 ±0.9	4.4 ±0.9	-0.7 ±1.3	(-9. ± 17.)	(-16. ± 30.)
		3	0.058 ±0.002	7.9 ±1.2	8.6 ±1.2	-0.7 ±1.6	(-9. ± 21.)	(-12. ± 28.)
		4	0.075 ±0.002	13.7 ±1.4	13.1 ±1.4	0.6 ±2.0	(8. ± 26.)	(8. ± 26.)
		5	0.075 ±0.002	21.0 ±1.6	18.5 ±1.6	2.6 ±2.2	34. ± 87%	34. ± 87%
		6	0.075 ±0.002	30.0 ±1.9	24.8 ±1.9	5.1 ±2.7	67. ± 53%	68. ± 53%
275	0.108	1	0.028 ±0.003	0.2 ±2.3	1.2 ±0.6	-1.0 ±2.3	(-9. ± 21.)	(-36. ± 84.)
		2	0.064 ±0.002	2.0 ±2.4	4.1 ±0.9	-2.1 ±2.6	(-19. ± 24.)	(-33. ± 41.)
		3	0.086 ±0.002	5.9 ±2.6	8.1 ±1.1	-2.1 ±2.9	(-20. ± 26.)	(-25. ± 33.)
		4	0.108 ±0.002	12.4 ±2.7	12.4 ±1.4	0.0 ±3.0	(-0.07 ± 28.)	(0. ± 28.)
		5	0.108 ±0.002	21.4 ±2.6	17.4 ±1.6	4.0 ±3.0	36. ± 76%	37. ± 76%
		6	0.108 ±0.002	30.8 ±2.6	23.3 ±1.9	7.4 ±3.2	68. ± 43%	69. ± 43%
273	0.139	1	0.035 ±0.006	1.3 ±2.1	1.3 ±0.6	0.0 ±2.2	(0.2 ± 15.)	(1. ± 62.)
		2	0.084 ±0.005	4.1 ±2.2	4.2 ±0.9	-0.1 ±2.4	(-0.4 ± 17.)	(-1. ± 29.)
		3	0.111 ±0.005	8.4 ±2.3	8.1 ±1.1	0.3 ±2.6	(2. ± 19.)	(3. ± 23.)
		4	0.138 ±0.004	14.2 ±2.4	12.4 ±1.4	1.9 ±2.7	(13. ± 20.)	(13. ± 20.)
		5	0.138 ±0.004	21.5 ±2.3	17.3 ±1.6	4.2 ±2.8	30. ± 66%	30. ± 66%
		6	0.138 ±0.004	30.3 ±2.3	23.1 ±1.9	7.2 ±3.0	52. ± 42%	52. ± 42%
271	0.157	1	0.039 ±0.009	1.3 ±1.5	1.0 ±0.6	0.3 ±1.6	(2. ± 10.)	(7. ± 40.)
		2	0.091 ±0.008	4.0 ±1.6	3.5 ±0.9	0.5 ±1.8	(3. ± 12.)	(5. ± 20.)
		3	0.123 ±0.007	8.1 ±1.6	7.0 ±1.2	1.1 ±2.0	(7. ± 13.)	(9. ± 16.)
		4	0.139 ±0.007	13.6 ±1.7	11.0 ±1.4	2.6 ±2.2	16.4 ± 84%	18. ± 84%
		5	0.147 ±0.007	20.4 ±1.6	15.3 ±1.6	5.0 ±2.3	32. ± 45%	34. ± 45%
		6	0.150 ±0.007	28.6 ±1.9	20.4 ±1.9	8.1 ±2.7	52. ± 33%	54. ± 34%

Table 11. Derivation of Conversion Factors for the Isoprene Experiments.

Run	Added (ppm)	Reacted (ppm)	IntOH (ppt-min)	Base ROG ConvR [a] (10^3 min-1)	d(O_3-NO) (ppm) Total	From Base ROG [b]	-Direct d(O_3-NO) Incremental (mol/mol) [c]	Reactivity- Mechanistic (ConvF)
277	0.076	0.075± 2%	30.0±1.9	33.2±3.0	1.167	0.993±0.110	2.3 ± 63%	2.3 ±63%
275	0.108	0.108± 2%	30.8±2.6	33.2±3.0	1.217	1.021±0.126	1.81 ± 64%	1.8 ±64%
273	0.139	0.138± 3%	30.3±2.3	33.1±3.0	1.262	1.004±0.119	1.85 ± 46%	1.9 ±46%
271	0.157	0.150± 5%	28.6±1.9	32.9±3.0	1.207	0.941±0.106	1.70 ± 40%	1.8 ±40%

[a] Conversion ratio from base case runs for the conditions of this experiment.
[b] Estimated from $ConvR^{base}$ x $IntOH^{test}$ as discussed in the text.
[c] $IR[d(O_3\text{-}NO)]^{direct} = [d(O_3\text{-}NO)^{test} - d(O_3\text{-}NO)^{from\ base\ ROG}]/[VOC]_0$.

The details of how the quantities on Tables 9-11 are derived, and the methods used to estimate their uncertainties, are discussed in Appendix A.

Representative plots of the mechanistic reactivity results are given in Figures 3-5. The two-hour and final d(O_3-NO) incremental reactivities and the final IntOH and direct incremental reactivities are plotted against amounts of isoprene added in Figure 3, and figures 4 and 5 show plots of the hourly d(O_3-NO), IntOH and direct mechanistic reactivities against time for each of the added isoprene runs. Results of model calculations using the SAPRC-91 mechanism (see above) are also shown.

A summary of the incremental and mechanistic reactivity results for isoprene is given on Table 12, where they can be compared with similar results for other selected VOCs. (A complete tabulation of comparable results of all VOCs studied using this approach is given in Appendix A.) It can be seen that isoprene is like the other alkenes studied in that it has a positive effect on NO oxidation, ozone formation and on OH radical levels, but that isoprene has a higher conversion factor than the other alkenes. Isoprene and the other alkenes differ from the alkanes in that they have positive effects on radical levels, yet the alkenes have smaller effects on radical levels than the alkylbenzenes. Isoprene has a comparable effect on radical levels as ethene and isobutene, and a smaller effect on radicals than trans-2-butene. However, because of its higher conversion factor (greater amounts of NO oxidized and ozone formed from the direct reactions of isoprene and its products) relative to the other alkenes, isoprene has a higher 6-hour d(O_3-NO) reactivity than does ethene or isobutene, and has almost as high a d(O_3-NO) reactivity as trans-2-butene.

Results of Model Calculations

The results of the model simulations of the isoprene reactivity measurements are shown on Figures 3-5, where they can be compared with the experimental data. As discussed above, model simulations were carried out using three

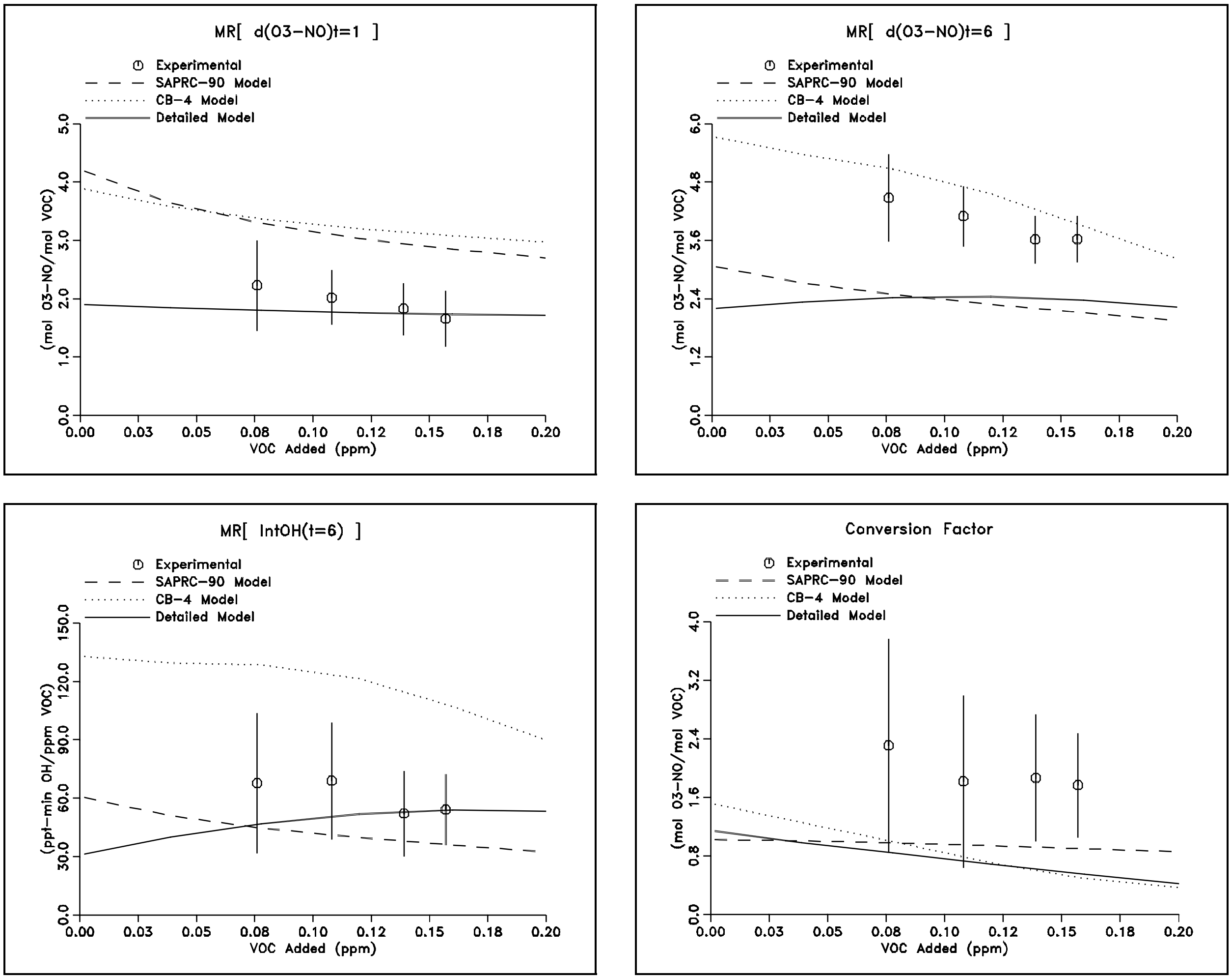

Figure 3. Plots of representative mechanistic reactivity results for isoprene against amounts of isoprene added.

isoprene mechanisms: the SAPRC-90 mechanism as documented by Carter (1990), the Carbon Bond IV isoprene mechanism (Gery et al., 1988), and a preliminary detailed isoprene mechanism we are developing for another program. The following results can be noted:

The SAPRC-90 isoprene mechanism predicts that the IntOH (i.e., the indirect) reactivities decline slightly with time, in contrast with the experimental results, where this increases with time. In particular, the IntOH reactivities are overpredicted early in the run, but are reasonably well predicted by the end of the run. The SAPRC-90 isoprene mechanism also systematically underpredicts the direct reactivities at all times in the runs. Since the d(O_3-NO) reactivities are the sum of the indirect (IntOH) and direct reactivi-

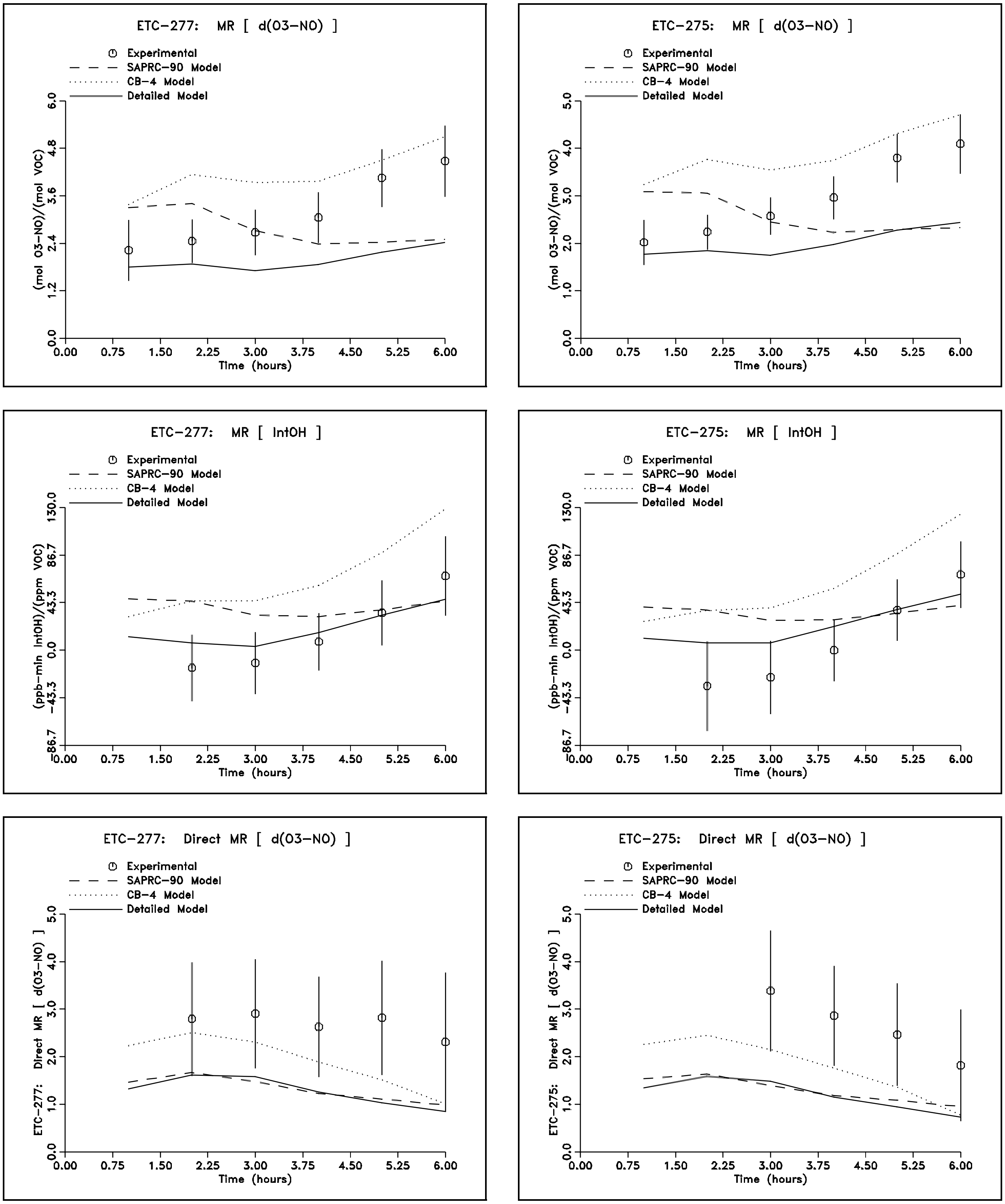

Figure 4. Plots of $d(O_3$-$NO)$ and IntOH mechanistic reactivity results against time measured in the added isoprene runs ETC-277 and ETC-275.

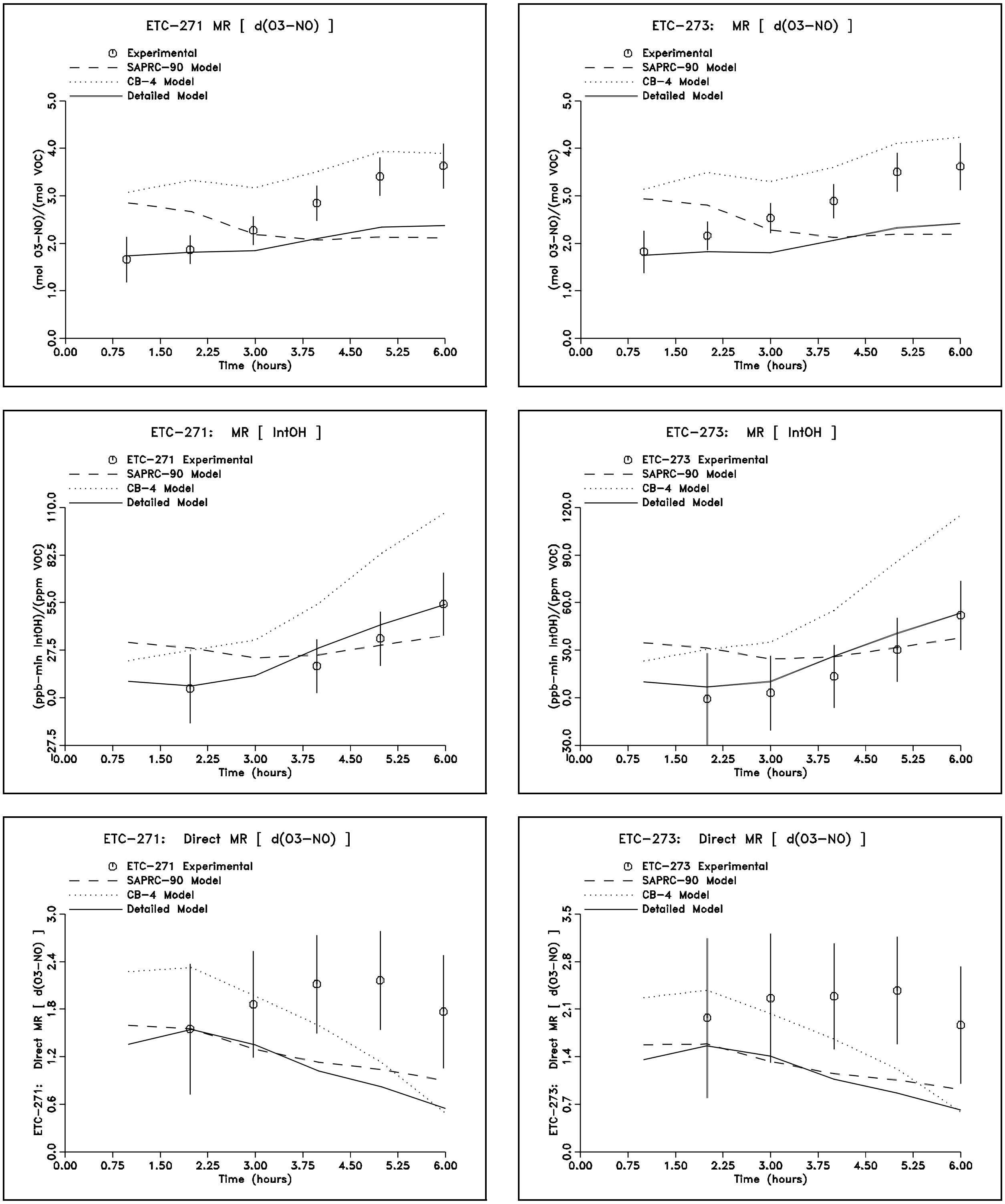

Figure 5. Plots of $d(O_3\text{-}NO)$ and IntOH mechanistic reactivity results against time measured in the added isoprene runs ETC-271 and ETC-273.

Table 12. Summary of Reactivity Results For Isoprene and Other Selected VOCs. (Quantities in parentheses are uncertainty estimates.)

Run	Added (ppm)	Reacted (ppm)	Reactivity: Incremental (mol O_3-NO/ mol added)		Reactivity: Mechanistic (mol O_3-NO/mol reacted) d(O_3-NO)	IntOH [a]	ConvF
					Isoprene		
277	0.076	0.075 (2%)	4.44	(20%)	4.5 ± 0.9	2.2 ± 1.2	2.3 ± 1.5
275	0.108	0.108 (2%)	4.06	(15%)	4.1 ± 0.6	2.3 ± 1.0	1.8 ± 1.2
273	0.139	0.138 (3%)	3.59	(14%)	3.6 ± 0.5	1.7 ± 0.7	1.9 ± 0.9
271	0.157	0.150 (5%)	3.49	(13%)	3.6 ± 0.5	1.8 ± 0.6	1.8 ± 0.7
					Ethene		
203	0.217	0.086 (29%)	0.912	(35%)	2.3 ± 1.0	2.0 ± 1.2	0.3 ± 1.2
199	0.386	0.172 (20%)	1.14	(17%)	2.5 ± 0.6	1.9 ± 0.8	0.7 ± 0.8
					Isobutene		
257	0.108	0.104 (2%)	2.73	(23%)	2.8 ± 0.6	2.4 ± 0.9	0.4 ± 1.0
255	0.195	0.192 (12%)	2.27	(19%)	2.3 ± 0.4	2.6 ± 0.6	-0.3 ± 0.7
253	0.207	0.205 (7%)	2.46	(15%)	2.5 ± 0.4	2.4 ± 0.5	0.0 ± 0.6
					trans-2-Butene		
309	0.069	0.068 (11%)	5.47	(21%)	5.5 ± 1.2	4.2 ± 1.5	1.3 ± 1.6
307	0.087	0.086 (35%)	5.09	(38%)	5.1 ± 1.9	4.5 ± 2.0	0.5 ± 1.5
					Ethane		
235	43.7	0.306 (6%)	0.0058	(26%)	0.8 ± 0.2	-0.6 ± 0.3	1.4 ± 0.3
					n-Octane		
239	1.55	0.064 (28%)	-0.243	(18%)	-5.9 ± 2.0	-9.7 ± 3.2	3.5 ± 1.4
237	1.66	0.098 (19%)	-0.235	(17%)	-4.0 ± 1.0	-5.9 ± 1.5	1.9 ± 0.8
					p-Xylene		
348	0.075	0.036 (3%)	2.63	(35%)	5.5 ± 1.9	5.1 ± 2.6	0.4 ± 3.2
346	0.080	0.039 (3%)	2.93	(31%)	6.0 ± 1.9	4.9 ± 2.4	1.7 ± 3.0
					135-trimethyl-Benzene		
251	0.045	0.042 (7%)	9.78	(17%)	10.4 ± 1.8	11.6 ± 2.6	-1.7 ± 2.8
249	0.047	0.045 (11%)	12.8	(16%)	13.3 ± 2.1	14.0 ± 3.0	-1.1 ± 3.3

[a] IntOH reactivities are expressed in terms of moles NO oxidized and ozone formed resulting from the change in IntOH caused by the addition of the VOC. The change in NO oxidized + ozone formed resulting from a given change in IntOH is estimated from the ratio $d(O_3\text{-NO})^{base}/IntOH^{base}$.

ties, these two factors together results in the d(O_3-NO) reactivities being overpredicted early in the run, and being underpredicted by the end of the run.

The Carbon Bond isoprene mechanism consistently overpredicts the IntOH reactivities throughout the runs, but also tends to underpredict the direct reactivities. However, it has less of a tendency to underpredict the direct reactivity early in the run. Because of these two factors, this mechanism significantly overpredicts the d(O_3-NO) reactivity early in the run, but by the end of the run the errors in the indirect (i.e., IntOH) and direct reactivity predictions tend to cancel out, and the mechanism only slightly overpredicts the final d(O_3-NO) reactivities.

The detailed isoprene mechanism performs significantly better than the other two mechanisms in the simulations of the effects of isoprene on radical levels, fitting the IntOH reactivities to within the experimental uncertainties throughout all four runs. However, it has a tendency to overpredict the initial IntOH reactivities and underpredict the final values, though to a far lesser extent than is the case for the SAPRC-90 mechanism. More significantly, the detailed mechanism performs no better than the SAPRC-90 mechanism, and slightly worse than the Carbon Bond mechanism, in fitting the direct reactivities, underpredicting them throughout the runs, except perhaps at the beginning of the runs. These factors result in the detailed mechanism simulating the d(O_3-NO) reactivities reasonably well initially, but significantly underpredicting them at the end of the run.

Thus, none of the three isoprene mechanisms we have considered are completely consistent with these data. The Carbon Bond mechanism appears to perform the best in simulating the effects of isoprene on the final ozone yield at the end of the run, but this is because of compensating errors in the predictions of direct and indirect reactivity. The SAPRC-90 mechanism, which represents isoprene in a manner similar to the RADM-II mechanism, is even less satisfactory than the Carbon Bond version, since it’s errors in the direct and indirect components do not tend to compensate. The detailed mechanism is perhaps the least unsatisfactory, since at least it predicts, to within the experimental uncertainty, the effect of isorpene’s reactions on OH radical levels. However, it is no better than the other mechanisms in predicting the relatively high direct reactivities of isoprene. As shown on Table 12, these data show that isoprene has a relatively high direct reactivity compared to the other alkenes, and none of the present mechanisms, even the most detailed, adequately explain this observation.

CONCLUSIONS

This study was successful in its objective of providing data concerning the amount of additional ozone formation resulting when isoprene is added to the emissions in already polluted atmospheres under conditions where ozone formation is most sensitive to VOCs. Information was also obtained concerning how much of that additional ozone was directly due to the reactions of isoprene and its products, and how much was due to the effect of the added isoprene on the amount of ozone formed from the reactions of the other VOCs which were present. Under the conditions of these experiments, isoprene was found to form approximately four molecules of ozone for each molecule of isoprene emitted and reacting in six hours, with approximately half of these being due directly to the reactions of isoprene and its reaction products, and the other half being due to the fact that the reactions of isoprene cause increased OH radical levels, resulting in more of the other VOCs present reacting to form ozone.

These experiments were carried out in conjunction with a much larger study where similar data was obtained concerning other VOCs, allowing the reactivity characteristics of isoprene to be compared with those for other VOCs. Isoprene is like the other alkenes in having positive effects on radical levels, giving it relatively high ozone reactivities under conditions where ozone is sensitive to VOCs, especially when compared to alkanes and other types of VOCs which have low mechanistic reactivities because their reactions suppress radical levels. The effect of isoprene on radical levels is comparable to ethene, propene (see Appendix A), and isobutene, and approximately half that of trans-2-butene. Thus, it is similar to other terminal alkenes in that respect. However, the direct reactivity of isoprene, i.e., the amount of NO oxidized and ozone formed directly from the reactions of isoprene and its products, is significantly higher than observed for the other alkenes studied. This results in isoprene having a comparable total reactivity under the conditions of these experiments to trans-2-butene, despite isoprene's lower reactivity relative to effects on radical levels. Thus, isoprene clearly has different reactivity characteristics from the other alkenes, at least in some respects.

The ultimate practical benefit of these data will come when the chemical mechanisms used in the airshed models are updated to take these results into account. These data were found to be inconsistent in a number of respects with predictions of the two isoprene mechanisms which represent the current state of the art for the airshed models which are presently in use. Perhaps the most widely used mechanism is Carbon Bond IV, which is implemented in the Urban Airshed Model (UAM) and the EPA's Regional Oxidant Model (ROM). Although this mechanism was found to give the best prediction of the three studied on the effects of isoprene on the 6-hour ozone in these experiments, this was found to be due to compensation of errors, since this mechanism underpredicted isoprene's direct reactivity and overpredicted its effect on radical levels. The SAPRC-90 isoprene mechanism, which is being implemented into a version of the UAM (Lurmann et al, 1991), and is very similar to the isoprene used in the RADM-II model (Carter and Lurmann, 1990; Stockwell et al., 1990), is even less satisfactory than the Carbon Bond version, significantly underpredicting both the direct and the overall reactivity of isoprene. Thus, the isoprene mechanisms in the currently used models clearly need to be updated.

Although the relatively poor performance of the Carbon Bond IV and SAPRC-90 isoprene mechanisms in simulating these data is of obvious concern to the users of the models incorporating them, it is perhaps not surprising given the approximations in these condensed mechanisms. Of greater concern from a standpoint of developing improved isoprene mechanisms for future models is the performance of a preliminary detailed isoprene mechanism we are in the process of developing. Although this detailed mechanism employs relatively few condensations, and attempts to explicitly represent the reactions of isoprene's major primary and secondary products, and although it simulates the available isoprene-NO_x and isoprene produce-NO_x chamber experiments significantly better than the other mechanisms we have tested, it was also found to be not completely consistent with the results of these reactivity experiments. In particular, although it — unlike the more condensed mechanisms — can simulate the effect of isoprene on radical levels within the uncertainty of the experimental measurements, it does not successfully simulate the relatively high direct reactivity observed for isoprene. Since this discrepancy in this mechanism's predictions of incremental reactivity tend to increase with reaction time, we suspect that this is likely due to problems with the representation of isoprene's major reactive products. However, this is still under investigation. The only definitive conclusion we can draw at the present time is that our current and most detailed theories about how isoprene reacts in the atmosphere cannot explain the isoprene reactivity data. More work in this area is clearly needed.

It is also important to recognize that this study does not provide all the data needed to adequately evaluate the reactivities of biogenic VOC emissions. In the first place, isoprene is not the only biogenic compound emitted in significant quantities, and comparable experiments are needed to test the mechanisms for the monoterpenes, which are even more uncertain. In addition, the present experiments are suitable only for testing the effects of isoprene on ozone formation under the relatively high NO_x conditions where VOCs have their greatest effects on ozone formation. While this is obviously important, it is also important that the ability of the mechanisms to predict reactivity be tested under conditions where NO_x is more limited. This is particularly true for biogenic VOCs, since their emissions tend to dominate in remote locations where NO_x is depleted or absent. Although the existing body of isoprene - NO_x - air experiments can provide useful data in this regard, experiments with the compound reacting in the absence of other VOCs do not always give a complete indication of the effect of a compound on ozone formation in an environment containing other reacting organic pollutants, as is usually the case in ambient atmospheres.

REFERENCES

Carter, W. P. L. and R. Atkinson (1987): "An Experimental Study of Incremental Hydrocarbon Reactivity," Environ. Sci. Technol., 21, 670-679

Carter, W. P. L. and R. Atkinson (1989): "A Computer Modeling Study of Incremental Hydrocarbon Reactivity", Environ. Sci. and Technol., 23, 864.

Carter, W. P. L. (1990): "A Detailed Mechanism for the Gas-Phase Atmospheric Reactions of Organic Compounds," Atm. Environ., 24A, 481-518.

Carter, W. P. L., and F. W. Lurmann (1990): "Evaluation of the RADM Gas-Phase Chemical Mechanism," Final Report, EPA-600/3-90-001.

Carter, W. P. L. (1991): "Development of Ozone Reactivity Scales for Volatile Organic Compounds", EPA-600/3-91/050, August.

Carter, W. P. L. and F. W. Lurmann (1991): "Evaluation of a Detailed Gas-Phase Atmospheric Reaction Mechanism using Environmental Chamber Data," Atm. Environ. 25A, 2771-2806.

Chang, T. Y. and S. J. Rudy (1990): "Ozone-Forming Potential of Organic Emissions from Alternative-Fueled Vehicles," Atmos. Environ., 24A, 2421-2430.

Dodge, M. C. (1984): "Combined Effects of Organic Reactivity and NMHC/NO_x Ratio on Photochemical Oxidant Formation -- A Modeling Study," Atmos. Environ., 18, 1657.

Dodge, M.C. (1990): "A Comparison of Three Photochemical Reaction Mechanisms," J. Geophys. Res. 94, 5121-5136.

Gery, M. W., G. Z. Whitten, and J. P. Killus (1988): "Development and Testing of the CBM-IV For Urban and Regional Modeling,", EPA-600/ 3-88-012, January.

Jeffries H. E., K. G. Sexton, J. R. Arnold, and T. L. Kale (1989): "Validation Testing of New Mechanisms with Outdoor Chamber Data. Volume 2: Analysis of VOC Data for the CB4 and CAL Photochemical Mechanisms," Final Report, EPA-600/3-89-010b.

Johnson, G. M. (1983): "Factors Affecting Oxidant Formation in Sydney Air," in "The Urban Atmosphere -- Sydney, a Case Study." Eds. J. N. Carras and G. M. Johnson (CSIRO, Melbourne), pp. 393-408.

Paulson, S. E. and J. H. Seinfeld (1992): "Development and Evaluation of a Photooxidation Mechanism for Isoprene," J. Geophys. Res. 97, 20,703-20,715.

Lurmann, F. W., M. Gery, and W. P. L. Carter (1991): "Implementation of the 1990 SAPRC Chemical Mechanism in the Urban Airshed Model," Final Report to the South Coast Air Quality Management District, Sonoma Technology, Inc., Report STI-99290-1164-FR, Santa Rosa, California.

Stockwell, W. R., P. Middleton, J. S. Chang, and X. Tang (1990): "The Second Generation Regional Acid Deposition Model Chemical Mechanism for Regional Air Quality Modeling," J. Geophys. Res. 95, 16343- 16376.

APPENDIX A

REPORT ENTITLED:

"ENVIRONMENTAL CHAMBER STUDIES OF MAXIMUM INCREMENTAL REACTIVITIES OF VOLATILE ORGANIC COMPOUNDS"

by

William P. L. Carter, John A. Pierce,
Irina L. Malkina, Dongmin Luo, and William D. Long

This report is now finalized and available as a separate volume. The full reference citation is given below. The report is available from the Coordinating Research Council in Atlanta GA, or can be downloaded by anonymous FTP from cert.ucr.edu, directory /pub/carter/pubs, file RCTRPT-1.PDF. (June 1, 1995.)

Carter, W. P. L., J. A. Pierce, I. L. Malkina, D. Luo and W. D. Long (1993): "Environmental Chamber Studies of Maximum Incremental Reactivities of Volatile Organic Compounds," Report to Coordinating Research Council, Project No. ME-9, California Air Resources Board Contract No. A032-0692; South Coast Air Quality Management District Contract No. C91323, United States Environmental Protection Agency Cooperative Agreement No. CR-814396-01-0, University Corporation for Atmospheric Research Contract No. 59166, and Dow Corning Corporation. April 1.